Metadata of the chapter that will be visualized online

ChapterTitle	Additive Processes for Metals	
Chapter Sub-Title		
Chapter CopyRight - Year	Springer Science+Business Media, LLC 2011 (This will be the copyright line in the final PDF)	
Book Name	MEMS Materials and Processes Handbook	
Corresponding Author	Family Name	**Arnold**
	Particle	
	Given Name	**David P.**
	Suffix	
	Division	Department of Electrical and Computer Engineering
	Organization	University of Florida
	Address	Gainesville, FL, USA
	Email	darnold@ufl.edu
Author	Family Name	**Saumer**
	Particle	
	Given Name	**Monika**
	Suffix	
	Division	Department of Microsystems Technology
	Organization	University of Applied Sciences
	Address	Kaiserslautern, Germany
	Email	monika.saumer@fh-kl.de
Author	Family Name	**Yoon**
	Particle	
	Given Name	**Yong-Kyu**
	Suffix	
	Division	Department of Electrical Engineering
	Organization	University at Buffalo, The State University of New York
	Address	Buffalo, NY, USA
	Email	ykyoon@buffalo.edu
Abstract	Metals are vital building blocks for MEMS. Pure metals and metal alloys are employed in microsystem design to achieve a wide array of functionality. Common examples include electrical conductors, mechanical structures, magnetic elements, thermal conductors, optical reflectors, and more. In this chapter, additive processes for metals are discussed in the context of their application in MEMS. Particular attention is paid to MEMS-centric processing technologies, where thick metal layers are often required. Basic guidelines are given for material selection, and fabrication recipes are provided as a starting point for process development.	

Chapter 3
Additive Processes for Metals

David P. Arnold, Monika Saumer, and Yong-Kyu Yoon

Abstract Metals are vital building blocks for MEMS. Pure metals and metal alloys are employed in microsystem design to achieve a wide array of functionality. Common examples include electrical conductors, mechanical structures, magnetic elements, thermal conductors, optical reflectors, and more. In this chapter, additive processes for metals are discussed in the context of their application in MEMS. Particular attention is paid to MEMS-centric processing technologies, where thick metal layers are often required. Basic guidelines are given for material selection, and fabrication recipes are provided as a starting point for process development.

3.1 Introduction

From the Bronze Age through the Iron Age, and even into modern times, metals have fueled technological growth and played a key role in shaping society. All but 25 of the 120 elements on the periodic table are considered metals, and many are naturally abundant on earth. Elemental metals are generally known to exhibit high electrical conductivity, high thermal conductivity, relatively high physical density, and good mechanical ductility. In addition, metals can be combined with each other or with nonmetals to form innumerable metal alloy combinations with diverse electrical, mechanical, magnetic, thermal, and optical material properties. The availability, adaptability, and functionality of metals make them one of the most widely used engineering materials, not only at the macroscale, but also for microscale applications.

AQ1 D.P. Arnold (✉)
Department of Electrical and Computer Engineering, University of Florida, Gainesville, FL, USA
e-mail: darnold@ufl.edu

R. Ghodssi, P. Lin (eds.), *MEMS Materials and Processes Handbook*,
MEMS Reference Shelf, DOI 10.1007/978-0-387-47318-5_3,
© Springer Science+Business Media, LLC 2011

UNCORRECTED PROOF

3.1.1 Overview

Metals are widely used for MEMS in many different functional roles. Metals are ubiquitously used as electrical interconnections for their high electrical conductivity. Metals also exhibit advantageous mechanical properties, so they are commonly employed as mechanical elements, both rigid structures and flexures. Metals are also good thermal conductors, and thus attractive for thermal applications. Certain metals exhibit ferromagnetic behavior and can be used to create or guide magnetic fields. For optical applications, metals are used to provide reflective, mirrorlike surfaces. Metal coatings are also used to encapsulate other materials, for example, to prevent oxidation or create hermetic seals, and thin interfacial metal layers act to enhance adhesion or prevent diffusion.

Material selection usually begins by identifying and prioritizing the desired material properties. For example, if a microstructure is intended as a mechanically strong electrical conductor, one may begin by searching for materials with high electrical conductivity and high elastic modulus. Fortunately, bulk metals and metal alloys have been widely studied for hundreds of years, and much of what is known about bulk material properties largely applies at the microscale. With the emergence of microelectronics, MEMS, and nanotechnology, there is also a growing wealth of knowledge about unique material behavior at the micro- and nanoscale.

Once a specific metal or class of metals is identified, the next step is to determine how to fabricate and integrate the material into a microdevice. Although bulk machining of metals is usually a top-down process (e.g. physical milling of a bulk piece of metal), micromachining of metals is usually bottom-up (atom-by-atom, layer-by-layer deposition). Herein lies a major complication. For macroscale applications, individual components are usually fabricated separately and then assembled together. The individual system components can be machined independently of one another. In MEMS fabrication, this is usually not the case; devices are manufactured in a sequential integrated fashion by selectively adding and subtracting layers on a planar substrate. This manufacturing approach places limitations on materials and structure geometries. Furthermore, microfabrication creates a complex interplay between the fabrication process and the resulting material properties. These topics are further discussed throughout this chapter.

Methods for metal deposition can be categorized into three groups: physical vapor deposition (PVD), chemical vapor deposition (CVD), and electrochemical deposition (ECD). For MEMS, PVD and ECD are more commonly used, and thus are the primary focus of this chapter. Although CVD finds widespread usage in semiconductor devices and integrated circuits for conformal deposition of thin metal films, it is not as popular for MEMS fabrication because of film thickness limitations and process complexity.[1]

The remainder of Section 3.1 discusses general tradeoffs for the various fabrication approaches available for depositing metals and metal alloys. Section 3.2 provides a more detailed discussion of PVD methods for metals, including evaporation, sputtering, and pulsed-laser deposition. Section 3.3 describes ECD methods, including both electroplating and electroless plating. Section 3.4 describes LIGA and UV-LIGA processes, a key technological advancement in the history of MEMS. Finally, Section 3.5 presents material properties and process selection guidelines for metals.

[1]See Chapter 2 (specifically Section 2.3) for general information on CVD.

3.1.2 Fabrication Tradeoffs

There are many fabrication-related tradeoffs that must be considered for micromachining of metals. The final material properties of a metal are often highly dependent on the film thickness, deposition method, and specific processing conditions. This creates interesting design/fabrication/integration challenges and compromises. In addition, because of these geometrical and process dependencies, the material properties for metal films reported in the literature vary widely. Thus, although basic starting recipes may be found (and many are provided below), some process development is usually required for fine-tuning of the metal properties to meet a specific need.

In addition to differing material properties, various fabrication methods yield different microstructural features and process integration issues. For example, evaporation usually results in poor step-coverage but high film purity. Sputtering, on the other hand, can provide good sidewall coverage, but with lower film purity. PLD often affords high deposition rates, but is usually limited in deposition area. In contrast to these PVD methods, electroplating and electroless plating rely on chemically "growing" the metals. This enables selective deposition (e.g. using photoresist masks) only where needed, thus avoiding additional process steps and time required for film patterning via post-deposition chemical etching[2] or liftoff.[3] In addition, the material waste (overage) associated with PVD can have significant cost implications, especially for thick layers of expensive precious metals.

The required film thickness also affects fabrication process selection. For example, thinner metal films may be used as coatings or as interfacial layers. In contrast, to better conduct heat or to provide heftier mechanical structures, thicker metal films may be required. Evaporation and electroless plating are better suited for thinner films (e.g. less than 1 μm), whereas thicker films demand the faster deposition rates afforded by sputtering, PLD, or electroplating. For commercial manufacturing, there are also numerous tradeoffs involving cost, throughput, reliability, and repeatability.

The deposition of alloys raises additional issues. Different alloy ratios are often required to enhance a material property such as electrical resistance, mechanical hardness, magnetic permeability, and the like. In cases where a very specific alloy

[2]See Chapters 7 and 8 for more information on chemical etching.

[3]See Chapter 9 (specifically Section 9.2.5.5) for more information regarding liftoff.

UNCORRECTED PROOF

ratio is required, stoichiometric control is a major consideration. Reliably maintaining a specific alloy ratio over long periods of time is critical for repeatable, large-scale manufacturing. In addition to repeatability and control, there is another important fabrication-related aspect for alloys: the ability (or inability) to vary the alloy ratio. This is especially important for process development and for fine-tuning of alloy composition. Moreover, deposition methods that permit on-the-fly alloy control can be used to create graded alloys, multilayers, or other complex structures.

The different metal deposition methods offer varying degrees of alloy control. Evaporation of alloys is often discouraged because of the disparate and highly temperature-dependent vapor pressures of different metal constituents. This makes control of alloys difficult with conventional evaporation systems. In contrast, sputtering and PLD permit deposition of many different alloys with fairly repeatable alloy control, but adjusting the alloy ratio requires changing the metal target. This can create time-consuming and costly process development cycles. For electroplating, the alloy ratio can sometimes be readily adjusted by varying the electroplating current density without strong influence on the properties of the deposit. Unfortunately, the alloy ratio may also be sensitive to other process conditions such as pH, temperature, or stirring, so repeatability is sometimes difficult. Electroless plating is less commonly used for alloy deposition because of the complex interdependent factors that determine the composition. See Table 3.1 for a general summary.

Table 3.1 General tradeoffs for metal deposition

Fabrication process	Deposition rate	Deposition area	Film purity	Alloy control	Equipment complexity
Evaporation	Slow	Very large	High	Poor	Moderate
Sputtering	Moderate	Large	Moderate	Good	High
PLD	Moderate	Small	High	Good	High
Electroplating	Fast	Large	Moderate	Fair	Low
Electroless plating	Moderate	Large	Moderate	Fair	Very low

3.2 Physical Vapor Deposition

Physical vapor deposition (PVD) methods rely on the physical transfer of metal atoms from a metal source to the wafer substrate, unlike chemical methods, which employ a chemical reaction. Different physical phenomena can be used to drive the process, as described below.

3.2.1 Evaporation

Evaporative deposition, or more commonly just "evaporation," is a fairly straightforward method for metal deposition. The basic concept is to heat a metal sufficiently to create a vapor, which diffuses and recondenses in solid form on other surfaces.

This process is usually performed in high-vacuum conditions (below 10^{-5} torr) so as to limit gaseous molecular scattering and to create a high-purity process environment. Note that, although the metal to be evaporated is obviously very hot, the wafer substrate usually remains at room temperature, unless intentionally heated or cooled. Also, because of the very low chamber pressures, the metal vapor tends to follow a straight path, leading to very directional deposition and poor sidewall coverage.

A typical system comprises a process chamber, a vacuum system, and a metal heating system, as shown in Fig. 3.1. Wafers are usually mounted upside down on a hemispherical chamber ceiling, which may include a planetary system to rotate the wafers for improved uniformity. The metal to be deposited – known as the "charge" – is placed in metal "boat" or ceramic crucible. The chamber is then closed and evacuated to a base pressure of 10^{-6} torr or lower. Then, the metal is heated usually to 500–2500°C (depending on the metal) to increase the vapor pressure. After a warm-up period, a physical shutter is used to precisely start and end the deposition onto the wafers. A quartz crystal microbalance (QCM) mounted inside the chamber monitors the deposition, and can provide feedback signals for automated control.

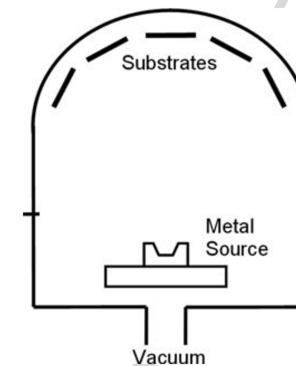

Fig. 3.1 Schematic of evaporation system

3.2.1.1 Thermal Evaporation

The simplest evaporation systems use joule heating to heat the metal charge. The dissipative heat can be created by direct conduction currents or magnetic-field-induced eddy currents. In the simpler conductively heated systems, high currents are passed through wound coils or a small metal boat (usually tungsten), inside of which sits the charge. The resistive heating of the boat facilitates deposition of relatively low-melting-point metals such as Ag, Al, and Au.

Evaporation of higher-melting-point refractory metals such as Ta, W, Mo, and Ti is challenging because these require very high temperatures to achieve reasonable vapor pressures and deposition rates [1]. Because of this, the use of metal boats and direct conductive heating may not be permissible. Instead inductive heating can be used where the metal sits in a ceramic crucible that is surrounded by a coil. RF

UNCORRECTED PROOF

excitation of the coil is used to induce eddy currents in the metal. This approach permits a wider range of metals, but the crucible itself may become very hot, which can result in contamination.

3.2.1.2 E-Beam Evaporation

Another configuration for evaporation uses a directed electron beam to bombard the metal charge. The electron beam source is usually underneath the metal charge. Strong magnetic fields are used to steer the electron beam in a 270° circular arc to impinge on the charge. Although more complicated, the advantage of this approach is that the electron beam heats a central portion of the charge: the outer area of the charge and crucible remain at lower temperatures, so as to minimize contamination.

3.2.1.3 Issues with Alloys

Evaporation of alloys with precise alloy composition can be quite challenging. The basic problem is that evaporation relies on heating to increase the vapor pressure and thus control deposition rate. The vapor pressure and deposition rate of an elemental metal are usually very sensitive to temperature, and different metals require vastly different temperature ranges for evaporation. For single-element deposition, precise control of the deposition rate is relatively unimportant, so long as the final film thickness is controlled. This is easily accomplished using a QCM to stop the deposition process at the predetermined film thickness.

Consider, however, deposition of a binary alloy. In a single-source system, a metal alloy can be used as the charge, but at a given temperature, the two metals in the alloy will evaporate at different rates, resulting in a different alloy ratio in the deposited layer. Attempts can be made to compensate for this, but impractically precise temperature control may be required. Another approach is to coevaporate different metals from independently heated crucibles. This allows independent control of the evaporation rates, but because of the temperature sensitivity of the evaporation process, and the inability to monitor the independent evaporation rates easily, precise alloy control remains very challenging. One alternative is to create a multilayer stack by alternating deposition of the constituent elements. After deposition, a heat treatment can be used to interdiffuse the metals to form the desired alloy. This approach, however, is more complicated, more time-consuming, and requires a substrate that can withstand the high-temperature postdeposition heat treatment.

It should be noted that graded alloys or multilayers can be easily achieved using a multisource evaporation system. However, because of the difficulty of alloy control, evaporation is better suited for pure metals or for metal alloys where precise composition is not necessary.

3.2.2 *Sputtering*

Sputtering is a physical process or phenomenon, where accelerated ions, usually Ar^+, knock out atoms in a solid target by bombardment in a potential gradient

environment. During the bombardment, momentum exchange occurs between the ions and the atoms of the surface of the target. The energized atoms are volatile and spread out as a vapor to land on the vicinity surface and the sample substrate. The sputtering process requires a vacuum environment, which is prepared by pumping out a stainless steel chamber enclosing the anode, the cathode, the target, the substrate, and so on. The chamber is evacuated to a base pressure of 10^{-6} torr or lower. Then a bombardment gas, usually Ar, is introduced to the chamber and maintained around 1–10 mtorr level. The Ar gas is ionized into Ar^+ by applying bias voltage between the anode and the cathode. Depending on the voltage waveforms used, the sputtering process is categorized as either direct current (DC) sputtering or radio frequency (RF) sputtering, as shown in Fig. 3.2.

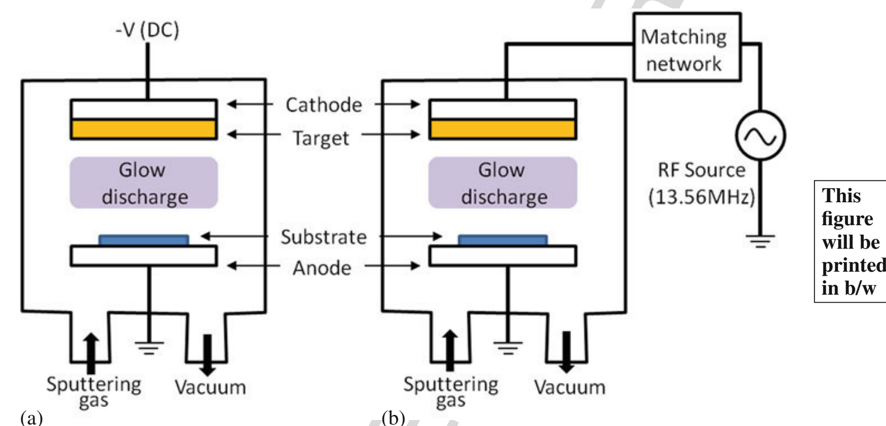

This figure will be printed in b/w

Fig. 3.2 Schematics of (**a**) DC and (**b**) RF sputtering systems

To obtain uniform thickness of a thin-film metal layer, mechanical movement such as rotation of the substrate holder can be used during the sputtering process. The rotational speed of the stage ranges from 10 to 30 rpm. The deposition rate is a function of many parameters including target-to-substrate distance, ion energy, the mass of the ion species, the mass of the target material, and the like [2].

3.2.2.1 DC Sputtering

For the sputtering of electrically conductive materials such as Al, Ti, Cr, Cu, Ag, Au, Pt, and W, a DC power source is used to energize the Ar^+ ions to bombard the target material placed on the cathode. The DC sputtering system, as depicted in Fig. 3.2a, consists of the DC power supply, cathode, a metal target attached to the cathode, Ar^+ plasma generated by high-voltage application, and an anode on which a sample wafer can be placed. The negatively biased metal target is bombarded by argon ions from the plasma, ejecting one or more metal atoms. Some of these ejected atoms are

UNCORRECTED PROOF

transported and deposited on the substrate wafers. The deposition rate is increased as the sputtering power is increased, however, too much power causes damage on the substrate. To counteract this effect, magnetron sputtering has been introduced to increase the deposition rate. A magnet placed behind the target creates a field that guides electron movement near the target, causing more efficient ionization of Ar without excessively high voltages.

3.2.2.2 RF Sputtering

As an alternative to the DC supply, RF power systems can be used, as shown in Fig. 3.2b. The RF sputtering system also requires a DC bias voltage to generate plasma. After plasma is generated, however, the major driving force acting on the argon ions is exerted by the alternating current source. Typically the 13.56 MHz industry, science, and medicine (ISM) frequency band is used. Because alternating currents can flow across dielectric materials, RF sputtering systems can deposit not only electrically conducting materials, such as metals, but also dielectric materials, such as SiO_2, Si_3N_4, and glass, which are not achievable with DC sputtering due to charging effects. Also, by reversing the electrical connections, the substrate can be bombarded as opposed to the metal target. This process is often used to clean the substrate surface before depositing the target material.

3.2.2.3 Step Coverage

In contrast to the evaporation process, sputtering provides reasonably conformal coatings on uneven surfaces. This is particularly useful for the metallization of three-dimensional (3-D) MEMS structures as well as the metal interconnect of integrated circuits. The step-coverage of a sputtered thin film in a via hole has been calculated [3, 4], where the profile shows a high deposition rate on the top surface and a low deposition rate on the sidewall. As a result, the sidewall thickness tapers down toward the bottom. For a very high aspect ratio, the bottom portion may not have sufficient metal coverage due to limited mass transfer into the narrow entrance of the via hole and the higher pressure environment in the chamber. This effect is depicted in Fig. 3.3. This kind of poor coverage is more significant in high-aspect-ratio vias or trenches as compared to high-aspect-ratio pillars or walls.

The step coverage can be improved by substrate heating to enhance surface diffusion or by applying an RF bias to the wafers to introduce surface bombardment resulting in redeposition on the sidewalls [1]. The heating approach may be applicable to the metal interconnect process for ICs, where the insulating layer is a temperature-tolerant material such as SiO_2, however, it may not be directly applicable for the metallization of 3-D MEMS structures where the structural material is often a temperature-intolerant polymer. Step-coverage of thin films for very high-aspect-ratio MEMS structures remains a challenging area. Alternatively, electroless plating may be used for the thin film metallization of such high-aspect-ratio polymeric structures.

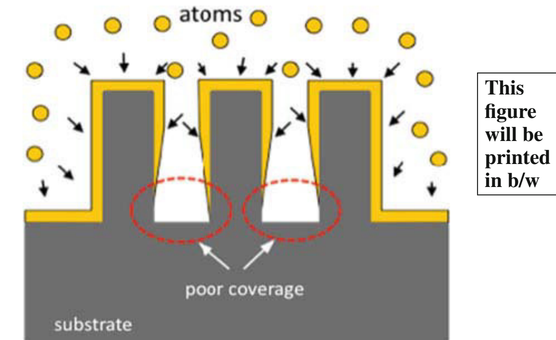

Fig. 3.3 Sputtered metal deposition in a densely placed high-aspect-ratio structure

This figure will be printed in b/w

3.2.2.4 Other Issues in Sputtering

One concern in thin-film deposition using sputtering (or evaporation) on a thick 3-D polymeric layer is that the residual solvent or moisture tends to degas under high vacuum conditions, resulting in poor adhesion between the polymer and thin-film metal layer. To prevent degassing effects, an additional hardbake step is recommended before the sputtering or evaporation process can be used.

One feature found in many sputtering systems is the ability to “clean” the substrate before the metal deposition by sputter etching. This cleaning step can improve adhesion of the metal. Sputter etching can be implemented either by reversing the electrical connections or by placing negative bias on the substrate with respect to the plasma, resulting in increasing ion bombardment on the substrate. Increasing the incident ion energy increases the adatom (Ar ion) mobility, which can aid in cleaning the deep sidewalls of a 3-D structure, thereby improving step-coverage in deep-etched features [5]. However, high sputter etch rates may cause substrate damage.

Although sputtering of alloy is commonplace, there are several important issues and approaches. In sputtering, the deposited film composition is usually fairly close to that of the bulk target, so alloys can be rather easily obtained. However, different elements in the target alloy may exhibit different sputter yields, causing composition variation. To achieve better control of stoichiometry, a multiple target system may be used, where the power of each target can be individually controlled to alter the final composition of the alloy layer. Also, by using a composite target with different regions of concentration or by changing electrical properties of the plasma, the composition of the deposited layer can be controlled [6].

Moreover, sputtered compounds can intentionally have a very different composition from the sputter target by adding reactive gaseous precursors during the deposition. Reactive sputtering is a process in which the normally inert sputter gas is replaced by an inert/reactive mixture [1]. For example, TiN, one of the most popular diffusion barrier layers in IC fabrication, can be deposited using reactive sputtering. By controlling the partial pressure of nitrogen in the sputtering system, the composition of TiN can be controlled.

UNCORRECTED PROOF

Stress is also an important issue for sputtered films. A thin film deposited on a substrate is subjected to either tensile or compressive stress as influenced by the base layer and deposition conditions. One component of the stress – known as extrinsic stress – is due to thermal expansion mismatch of the film with the substrate. This stress may be significant if the wafer temperature varies (intentionally or unintentionally) from room temperature during the film deposition. In addition, large intrinsic stresses may also occur depending on deposition rate, film thickness, and the background chamber environment. In many cases, efforts are made to minimize these stresses. Alternatively, for MEMS devices, these stresses can be put to good use to realize devices such as bimorph actuators or stress-engineered 3-D structures [7, 8].

3.2.3 Pulsed Laser Deposition

Pulsed laser deposition (PLD) is another method for depositing metals, although much less often used for MEMS. As shown in Fig. 3.4, the system uses a high-energy laser beam (typically 10^8 W/cm^2) to strike a metal target within a vacuum chamber. The laser beam melts, evaporates, and ionizes a region of the target. This ablation process creates a vapor plume that transfers material to the sample wafer.

One major advantage of PLD for MEMS applications is precise stoichiometry/composition control and relatively fast deposition rates. Ideally the deposited material possesses the same chemical composition as the metal target. High quality crystalline deposits are also possible with substrate heating. The biggest drawback is that most PLD systems can only provide uniform deposition over a small surface area, sometimes only about one square centimeter. This decreases the utility of PLD for volume manufacturing. Despite this drawback, PLD finds application where

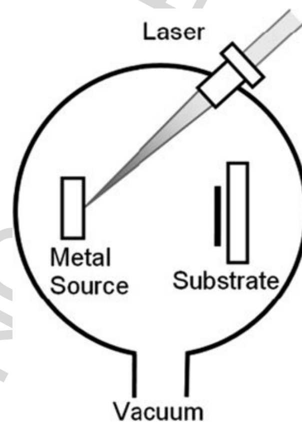

Fig. 3.4 Schematic of pulsed laser deposition system

precise stoichiometric control is paramount, especially for complex multielement materials. For metallic systems, this alloy control is beneficial for realizing high-performance magnetic materials and superconductors. PLD also finds widespread application for many other complex nonmetallic films, such as oxides, nitrides, and semiconductors.

The exact process and resulting film composition and structure are dependent on the laser parameters, chamber pressure/atmosphere, sample temperature, and sample surface quality. The complex physical and chemical interactions are the subject of ongoing research.

3.3 Electrochemical Deposition

Electrochemical deposition involves the reduction of metal ions from aqueous, organic, or fused-salt electrolytes. The reduction of metal ions M^{z+} in aqueous solution is represented by

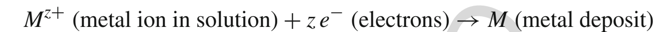

$$M^{z+}\ (\text{metal ion in solution}) + z\,e^{-}\ (\text{electrons}) \rightarrow M\ (\text{metal deposit})$$

Two processes can be used to provide the electrons for the reduction reaction: (1) electroplating (or electrodeposition), where an external power supply provides the electrons, or (2) electroless deposition, where a reducing agent provides the electrons.

In MEMS electrochemical deposition is commonly used to deposit surface coatings, or in the case of electroforming, for producing an entire microstructure or device. In electroforming, microstructured molds of different materials (e.g., polymers/resist, silicon) are electrochemically filled with metals such as nickel, copper, gold, or various metal alloys. More details can be found in Section 3.4.

3.3.1 Electroplating

The material properties of electroplated metals or alloys are strongly influenced by the chemistry of the electrolyte (e.g., type and concentration of ions, pH, type of additives), the physical parameters of the process (e.g., temperature, fluidics, current), and the property of the substrate (surface quality, shape). Depending on the metal to be plated and/or on the shape of the desired microstructures, the electroplating process has to be adapted to the specific application. The basics of electrochemical deposition can be found in several excellent books (e.g., [9–11]) and are summarized in this section. In addition, starting recipes are provided for some of the most common electroplated metals for MEMS: nickel, copper, gold, and some nickel alloys.

3.3.1.1 Electrochemical Reactions

The general setup and operation of an electrochemical deposition cell are shown in Fig. 3.5. Two electrodes are immersed into an electrolyte. By applying an electric

current, reduction (electron uptake) takes place at the cathode, and oxidation (electron liberation) occurs at the anode. In the case of electroplating, the substrate serves as the cathode, and metal ions are reduced to form a solid lattice. The anode can be soluble, meaning it is dissolved via oxidation during the electroplating process. The two partial reactions are expressed by the following equations.

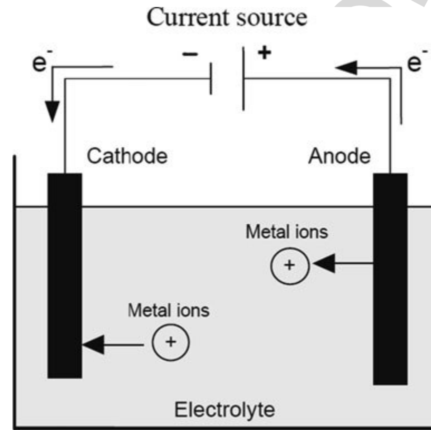

Fig. 3.5 Schematic of a general electrochemical deposition cell (using soluble anode)

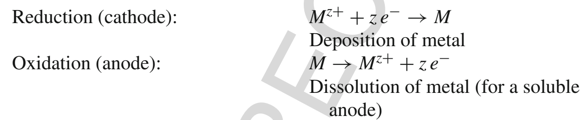

Reduction (cathode):	$M^{z+} + z\,e^{-} \rightarrow M$ Deposition of metal
Oxidation (anode):	$M \rightarrow M^{z+} + z\,e^{-}$ Dissolution of metal (for a soluble anode)

The steady oxidation of the anode (a metal to be deposited) ensures a constant replenishment of metal ions in the electrolyte. Sometimes inert anodes such as platinum are used, for example, in gold electroplating. In this case, replenishment of metallic ions in the electrolyte is solely provided by manual addition of metal salts to the plating bath.

The theoretically deposited mass m_{theo} can be calculated from the electrochemical Faraday's law as

$$m_{\mathrm{theo}} = \frac{M^{*}I^{*}t}{z^{*}F} \tag{3.1}$$

where M = Molar mass the deposited metal; I = Current; t = Time z = Valency; F = Faraday constant

Other reactions also can occur due to decomposition of water. By the oxidation of water, oxygen gas can be produced at the anode. By the reduction of water, hydrogen

UNCORRECTED PROOF

gas can be released at the cathode. Other components of the electrolyte can also react at the electrodes. The overall current is thus distributed to these different reactions. The percentage of the total current associated with the reduction of metal is defined as the cathodic current efficiency γ and can be calculated by the quotient of the effective deposited mass m_{eff} and the theoretical deposited mass m_{theo},

$$\gamma = \frac{m_{\mathrm{eff}}}{m_{\mathrm{theo}}}. \tag{3.2}$$

If hydrogen production at the cathode cannot be suppressed, it usually severely reduces the current efficiency of the deposition process. Another adverse effect is the rise of the pH at the electrode surface, which leads to the buildup and incorporation of metal hydroxides into the deposits, leading to a brittle deposit. The accumulation of hydrogen bubbles, which adhere on the surface, can also cause pores in the deposit.

3.3.1.2 Deposition Process

In the bulk electrolyte, cations are enclosed in a complex shell. This complex shell consists of water molecules (hydration shell) or other complexing agents such as sulfite or cyanide. Before applying a current, the ion concentration is homogeneous at the electrode surface and in the bulk solution. When applying a current, the metal ion is consumed at the electrode, and this depletion region extends farther away into the bulk as the deposition proceeds.

Movement of the complexed metal ions in the electrolyte is governed by three different mass transport mechanisms: migration, convection, and diffusion. In most deposition processes the conductivity of the electrolyte is relatively high, and the applied potentials are moderate. As a consequence, most of the electrical field drops across the electrical double layer in front of the electrodes, and field-induced migration is minimal. Therefore the predominant transport mechanisms are usually convection (due to stirring or agitation), which dominates in the bulk electrolyte, and diffusion, which dominates near the surface of the electrodes.

The reduction of the metal ions at the cathode is very complex and can be divided into four parts: (1) diffusion of the solvated or complexed metal ions from the bulk solution to the electrode surface, (2) dehydration and transport of the cations through the electric double layer, (3) cationic reaction at the solution–solid interface (ion uptake and electron transfer), and (4) surface migration and incorporation of the adsorbed metal atoms into the metal lattice. Figure 3.6 depicts the overall process.

The ion diffusion is described as follows. The region immediately next to the cathode is characterized by a fictitious Nernst diffusion layer, where the gradient of ion concentration is assumed constant, as shown in Fig. 3.7. The thickness of this layer δ is strongly influenced by convection (agitation) in the electrolyte, but is typically on the order of tens to hundreds of micrometers. In stirred electrolytes the thickness of the diffusion layer will be determined by this forced convection, whereas in unstirred electrolyte baths the diffusion layer increases with time.

UNCORRECTED PROOF

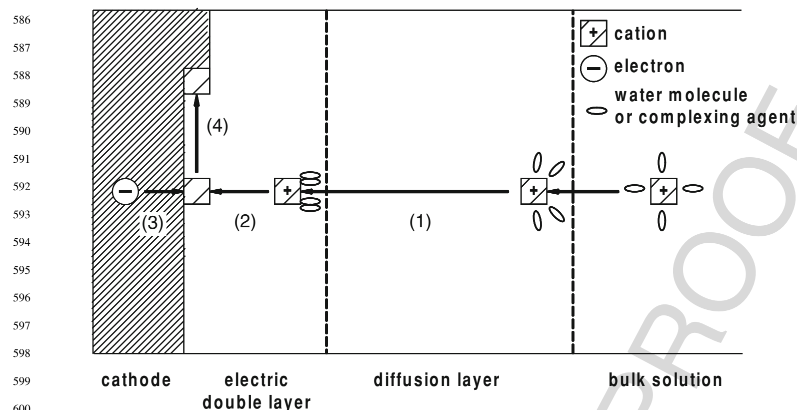

Fig. 3.6 Schematic diagram of the electrochemical deposition process

The deposition rate can be enhanced by increasing the current density, up until the ion concentration at the cathode approaches zero. The current density at which this occurs is called the limiting current density. The limiting current density (and hence maximum deposition rate) can generally be increased by increasing the cation concentration; by increasing the temperature, thus increasing the diffusion coefficient; and by increasing the convection (e.g., stirring the solution), resulting in a smaller diffusion layer. Modifying the electrolyte chemistry, especially via complexing agents, can also influence the limiting current density.

In the case of pulse-plating, the pulse current density is limited by the depletion of ions in the pulsation layer, whereas the average current density is limited by the concentration gradient in the outer stationary diffusion layer. Thus two diffusion layers can be defined: a pulsation layer in the immediate vicinity of the cathode and a stationary layer up to the point where the mass transfer is controlled by convection.

Once the cations reach the cathode surface by means of mass transfer, there is another barrier to overcome before they lose charge and are incorporated into the crystal lattice. That barrier is called the electric double layer. The simplest model of the double layer structure is given by the Helmholtz model, as depicted in Fig. 3.8. The double layer represents an organized arrangement of positive ions from the solution to compensate for the negative charges on the surface, forming an interface region similar to a parallel plate capacitor. The thickness of this layer is on the order of a few nanometers [12]. The cations to be deposited have to penetrate through the electric double layer, where they shed their hydration (or complex) shell. Then they acquire electrons in the reduction process and become adsorbed adatoms.

The final step in the formation of a crystalline metal deposit is the incorporation of the adatoms into the lattice. The adatoms are preferentially incorporated at active lattice sites such as grain boundaries, imperfections, or pre-existing built-up adatom

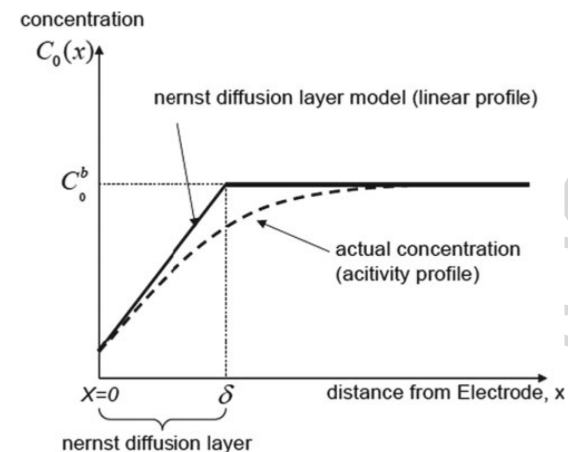

(a)

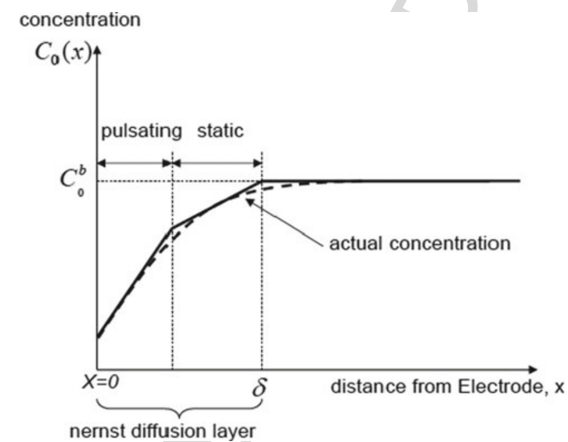

(b)

Fig. 3.7 Concentration of metal ions as a function of distance from the cathode (**a**) for direct current plating and (**b**) for pulse current plating

clusters on the surface. If the adsorption of an adatom ensued away from an energetically stable position, surface diffusion may transport the adatom to another active lattice site on the surface. The process of either building new grains (nucleation) or contributing to the growth of existing grains defines the formation of metal deposits in electroplating. Additional inhibitors in a plating bath can influence this nucleation

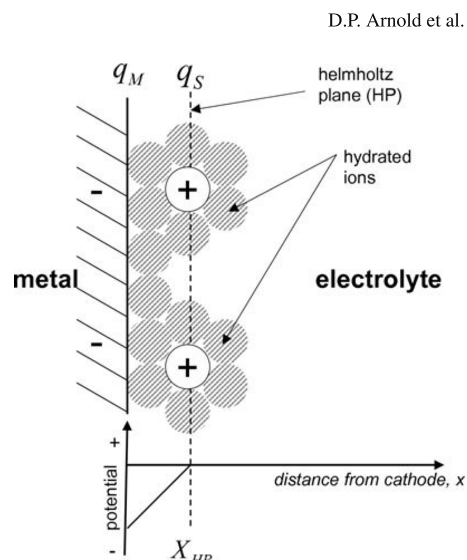

Fig. 3.8 Helmholtz model of the electric double layer. X_{HP} outer Helmholtz plane; q_M^- negative-charged metal surface; q_S positive-charged solution side of the interface

and therefore the growth processes that affect the properties of the deposit such as hardness, internal stress, and so on.

3.3.1.3 Overpotential

In the equilibrium condition (absence of external current), the potential of an electrode is denoted as E_h. As a result of a current flowing through the electrolyte the potential of the given electrode is changed to E. The difference between these two potentials is defined as overpotential

$$\eta = E - E_\mathrm{h} \tag{3.3}$$

The overpotential arises from the different electrochemical mechanisms associated with the reactions and movement of the ions or adatoms. The total overpotential is the sum of the individual overpotentials associated with each of these mechanisms. As a result, any one can be rate-determining for the electrodeposition. The diffusion overpotential η_diff arises due to mass transport through the diffusion layer. If this step is the slowest, the reaction is called diffusion-controlled. The activation overpotential η_act is associated with transfer of ions and electrons across the electric double layer and the transfer of the electrons. Therefore η_act is directly related to the electrode material. If the ion and electron transfer at the metal–solution interface is the most inhibiting step, the process is considered activation-controlled. The process by which the uncharged adatoms either form new grains or contribute to the growth of existing grains is associated with the crystallization overpotential η_crys. Ohmic

UNCORRECTED PROOF

overpotential η_ohm stems from the resistivity of the electrolyte. Although the contribution of each overpotential deserves consideration, the activation overpotential or the diffusion overpotential usually dominates.

3.3.1.4 Bath Composition

Every electrolyte contains metal salts. In addition, different inorganic or organic substances are added to improve either the performance of the electrolyte solution (e.g., conductivity) or the deposit quality (e.g., hardness, internal stress). Still other additives can be used for specific purposes. For example, saccharin is used to reduce the internal stress of nickel deposits [13], bromide is used for nickel anode activation [14], and As(III)-salt is used for brightening, grain-refining, and hardening of gold deposits [15]. Table 3.2 lists some typical additives and their function.

Table 3.2 Example chemical constituents of electrolyte solutions and their function

Type of substance	Function	Example
Metal salt	Provide metal ions	Ni(II)-sulfamate, Cu(II)-sulfate
Wetting agent (surfactant)	Reduce surface tension of electrolyte	Laurylsulfate, Fluorinated alkylsulfonates
Weak acid	Buffer the pH	Boric acid
Complexing agent	Stabilize electrolyte Influence selectivity of deposition process in alloy plating	1,2-Ethylendiamine Citrate
Salt	Increase conductivity of electrolyte	Sodium chloride
Brightener	Enhance or cause a bright surface of the deposit	Thiourea
Leveler	Reduce the surface roughness of the deposit	Coumarin

3.3.1.5 Current Waveform

In electroplating, besides the simple direct current, a variety of current modulations can be applied, such as triangular-, sawtooth-, or rectangular-shaped waveforms. Rectangular waveforms can be further divided into two characteristic variants: unipolar and bipolar current waveforms, both of which are commonly used. Table 3.3 illustrates the current-time-function of direct current, pulse forward current, and pulse reverse current. These current modulation schemes affect the plating mechanism and thus the chemical and microstructural properties of the deposited layer [16].

As can be seen in Table 3.3, the simplest case is the direct current mode. In contrast, the current waveform for pulsed electrodeposition (forward current) consists of cathodic pulses (t_c), separated by a current pause (t_p). Pulse reverse electrodeposition consists of a cathodic pulse (t_c), followed by an anodic pulse (t_a), where the current is reversed for a short time. In addition, the cycle can be extended

UNCORRECTED PROOF

Table 3.3 Current waveforms for direct current, forward current, and pulsed reverse plating[a]

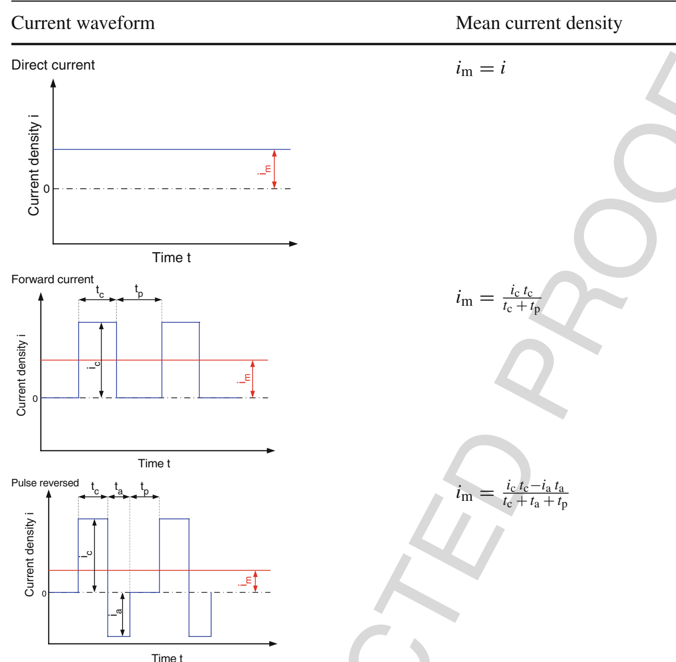

Current waveform	Mean current density
Direct current	$i_m = i$
Forward current	$i_m = \frac{i_c t_c}{t_c + t_p}$
Pulse reversed	$i_m = \frac{i_c t_c - i_a t_a}{t_c + t_a + t_p}$

[a]The parameters defining a cycle are: i = current density, i_m = mean current density, i_c = cathodic current density, i_a = anodic current density, t_c = duration of the cathodic pulse, t_a = duration of the anodic pulse, t_p = duration of the pulse pause

This figure will be printed in b/w

by a pulse pause (t_p). During the cathodic pulse, metal ions are deposited on the cathode surface. Areas where field lines are concentrated are plated preferentially. Conversely, metal is preferentially removed in those areas during the anodic cycle. As shown later, the relative field strengths depend on the absolute current value. Hence, applying pulse reverse currents can result in a planarization of the deposit.

In pulse plating, a mean current density (i_m) can be defined, using the amplitudes and durations of the various pulses. This value represents the average charge density transferred during one cycle, which governs the deposition rate. Note that in order to generate the same mean current density as in the direct current case, significantly higher amplitude forward pulse current densities have to be applied.

The advantages of pulse plating have been studied extensively. Various metal alloy compositions have been optimized for morphology, magnetic properties, or mechanical properties (e.g. [17–20]). In the fabrication of printed circuit boards (PCBs), pulse reverse electroplating of copper is used in order to attain a uniform

UNCORRECTED PROOF

filling of small vias and trenches. Pulse reverse methods can, to some extent, reduce the need for certain chemical additives and thus make bath control simpler.

3.3.1.6 Equipment

Various equipment can be used for electroplating, ranging from very simple to very complex. For laboratory use, the setup can be very simple, as shown in Fig. 3.9. This setup consists of a glass beaker, which contains the electrolyte solution. The electrolyte is stirred by a magnetic bar and heated by a hotplate. A temperature regulator connected to the hotplate automatically controls the temperature. A metal plate or titanium basket filled with metal pellets is used as the anode. An inert gas inlet for nitrogen or argon is sometimes used to prevent oxidation of the electrolyte. The power supply should be equipped with a pulse module to enable pulse plating if necessary. An oscilloscope may also be used to monitor the applied pulses.

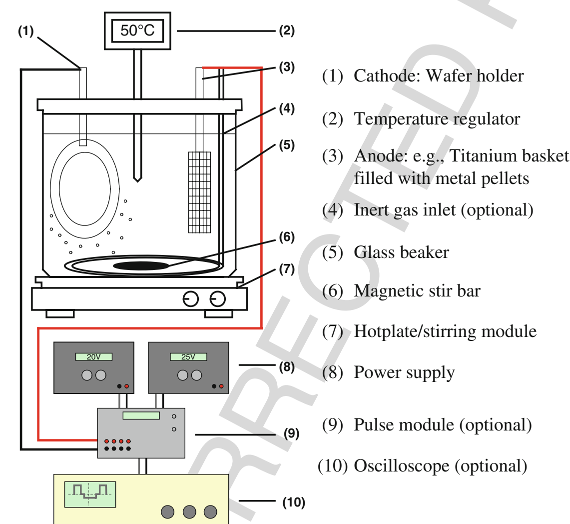

Fig. 3.9 Schematic of a laboratory-scale electroplating unit

This figure will be printed in b/w

An example of a more complex and commercially available electroplating unit is shown in Figs. 3.10 and 3.11. It holds a larger volume of electrolyte than that of a simple lab setup and includes monitors for liquid level, pH, and additives, as well as a continuous filtration and a dummy plating cell for cleaning of the electrolyte. Filtration rids the electrolyte of particles, which can interfere with the deposit. Dummy plating is used to deposit trace cation impurities on a dummy substrate before plating on the target substrate. For large-scale manufacturing, continuous filtering, salt replenishment, and pH maintenance are important issues. Also, some

UNCORRECTED PROOF

This figure will be printed in b/w

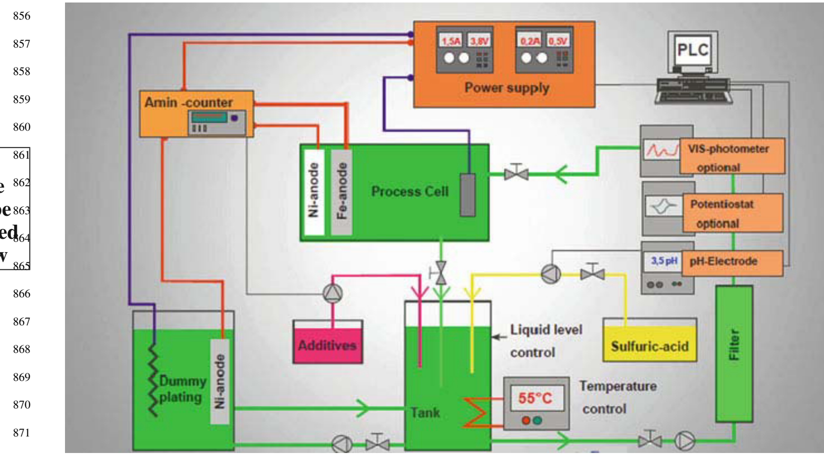

Fig. 3.10 Schematic of a commercially available Ni–Fe electroplating system (Reprinted with permission. Copyright 2009 M-O-T, Germany)

This figure will be printed in b/w

(a)

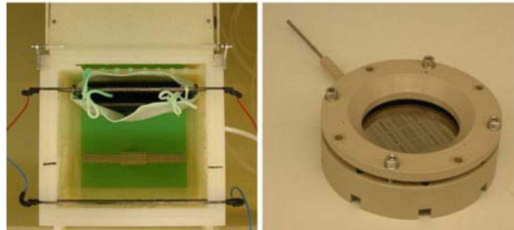

(b) (c)

Fig. 3.11 Commercially available electroplating unit for use in a cleanroom: (**a**) plating facility for cleanroom; (**b**) process cell with anode; (**c**) holder for cathode (Si wafer) (Reprinted with permission. Copyright 2009 M-O-T, Germany)

SPB-140376 Chapter ID 3 October 29, 2010 Time: 08:22pm Proof 1

baths may generate gaseous byproducts, so exhaust of these gases should also be considered.

3.3.1.7 Process Flow

A general overview of the electroplating process flow is shown in Fig. 3.12. The cleaning procedure has to be adapted to the substrate. Often a rinse with deionized water and a subsequent drying with nitrogen gas are sufficient for obtaining a particle-free surface. Weighing of the substrate before and after electroplating is necessary to calculate the current efficiency, which is an important value to estimate the process reproducibility. To ensure good performance and repeatability, process temperature, electrolyte circulation, and bath chemistry should be controlled accurately. Control of the pH is also crucial.

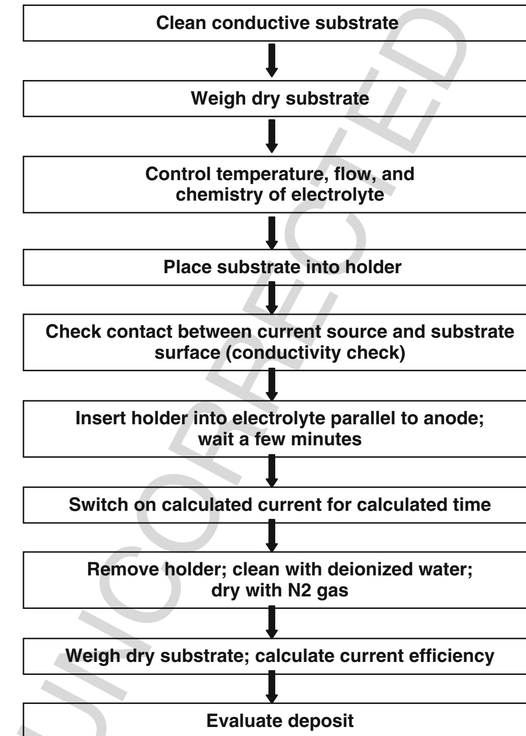

Fig. 3.12 Process flow for electroplating

UNCORRECTED PROOF

3.3.1.8 Nickel

Nickel electroforming is a well-established process for fabrication of microdevices and mold inserts [13, 14, 21–24]. The standard plating baths are based on nickel sulfamate. Boric acid is used as a pH buffer, and wetting agents (surfactants) are used to enable electrolyte penetration into micropatterned structures. An unwanted side reaction is the reduction of hydrogen ions to hydrogen gas according to the following equation.

$$\text{Hydrogen formation}: \quad 2\,H^{+} + 2e^{-} \rightarrow H_2(g)$$

As a result the current efficiency is not 100%, because some of the electrons are used to reduce the hydrogen ions instead of the metal ions. Also the concentration of hydrogen ions decreases, which changes the pH. The release of hydrogen gas can also form bubbles that cause pores in the deposit. Therefore a pH-buffering agent (e.g., boric acid) and a surfactant to enable gaseous hydrogen to escape during electroforming are crucial for the nickel electrolyte.

The electrolyte formulation and operation parameters can be modified for specific fabrication environments or according to the desired properties of the deposit. Some electrolytes contain additional additives such as stress reducers (e.g., saccharin). To enhance the electrical conductivity of the electrolyte and the solubility of the anode, chloride or bromide is used. Also the current density and current waveform are modified to vary the Young's modulus or hardness of the deposit [25].

Normally sulfur-depolarized nickel pellets are used as the anode material, but a high-purity nickel plate may also be used. A large surface area compared to the cathode and the generally good solubility of nickel result in a low anodic overpotential for most nickel electrolytes. Two typical nickel sulfamate electrolytes suitable for microfabrication are listed in Table 3.4.

Table 3.4 Example nickel sulfamate electrolytes used for microfabrication

Bath constituents and parameters	1	2
Nickel sulfamate ($Ni(NH_2SO_3)_2 \cdot 4H_2O$) (g/L)	105–110	80
Nickel(II)-bromide ($NiBr_2 \cdot 3H_2O$) (g/L)	0–5	
Boric acid (H_3BO_3) (mL/L)	40	30
Perfluorinated alkylsulfate (2 % solution) (wetting agent) (mL/L)	10	
Additive K (wetting agent) (mL/L)		5
Saccharin ($C_7H_4NNaO_3S \cdot 2H_2O$) (mg/L)	0–20	
pH	3.8	3.2
Temperature (°C)	50	40
Cathodic current density (A/dm^2)	1.0	0.1–2
Anode material	S-Ni pellets in a Ti basket	
Growth rate	10 μm/h	
References	[13]	[14]

3.3.1.9 Copper

Copper electroplating is used for manufacturing of microdevices and for auxiliary or sacrificial layers [13, 26]. The most common bath is an acidic sulfate-based electrolyte, which can be used at room temperature and is easy to maintain. For a good quality of deposit, organic chemicals are used as leveling agents, but this makes the maintenance of the electrolyte more complicated. Alternatively, copper fluoroborate is used as the Cu salt [27]. For details see Table 3.5. For formation of integrated circuit interconnects, a different copper plating process is used. Three or four component additive mixtures in the electrolyte combined with pulse plating facilitate the superfilling of via holes and trench lines during the plating process. For further details refer to [28].

Table 3.5 Example copper electrolytes used for microfabrication

Bath constituents and parameters	Copper sulfate-based	Copper fluoroborate-based
Copper (II)-sulfate ($CuSO_4 \cdot 5H_2O$) (g/L)	15–25	
Copper (II)-fluoroborate ($Cu(BF_4)_2$) (g/L)		60
Sulfuric acid (H_2SO_4, 98%) (mL/L)	200–250	
Fluoroboric acid (HBF_4) (mL/L)		13
Boric acid (H_3BO_3) (mL/L)		12
Sodium chloride (NaCl) (g/L)	0.06–0.1	
Wetting agent (mL/L)		3
Cuprostar LP1 (leveler) (mL/L)	5	
pH		0.7–1.0
Temperature (°C)	20–25	20–25
Cathodic current density (A/dm^2)	1–4	6–12
Anode material	Phosphorus depolarized copper	Copper (99.9% Cu)
Growth rate (μm/h)	12.5–50	
References	[13]	[27]

3.3.1.10 Gold

Gold has some outstanding properties, including very high conductivity, high ductility, excellent corrosion resistance, and good biocompatibility. Gold microstructures are used as metallic parts in microoptics, microfluidics, and micromechanics; for mask absorber structures in LIGA-technology; and for the fabrication of electrical contacts in the electronic industry.

Two kinds of gold are used in plating: soft gold (pure gold) and hard gold (gold alloy). Soft gold is used for metalizing bonding pads and for fabricating microbumps on silicon IC chips and ceramic packaging boards. Hard gold is used as a contact material on electrical connectors, printed circuit boards, and mechanical relays. For

UNCORRECTED PROOF
UNCORRECTED PROOF

hard gold, alloying metals such as Co, Ni, or W are used. Further aspects of gold plating processes in the electronic industry are reviewed by [29].

For electrolytic gold plating, three different types of baths are commonly used: sulfite-based electrolytes with a neutral or alkaline pH; thiosulfate-sulfite-based electrolytes with a weak acidity; or cyanide-based electrolytes with a range of pH from weakly acidic to strongly basic. Noncyanide baths are preferred because they are non-toxic and more compatible with conventional positive photoresists. Table 3.6 shows an overview of gold electrolytes suitable for microfabrication. In Table 3.7 some sulfite-based electrolytes are described. In all cases, a platinated titanium mesh is used as an insoluble anode. Specific skills are needed for mixing the chemicals to obtain a stable electrolyte. The authors recommend purchasing a complete electrolyte solution from a commercial vendor.

Table 3.6 Comparison of gold electrolytes suitable for microfabrication

Bath type	Gold complex	Current densities (A/dm^2)	Advantages/disadvantages	References
Sulfite-based	$[Au(SO_3)_2]^{3-}$	0.1–0.4	High current efficiency Very sensitive to process parameters	[30– 32]
Thiosulfate-sulfite-based	$[Au(S_2O_3)_3]^{3-}$ $[Au(SO_3)_2]^{3-}$	0.5	Good bath stability High internal stress of deposit	[29, 33, 34]
Cyanide-based	$[Au(CN)_2]^-$	0.2–0.5	Good bath stability High toxicity Instability of some resists (tend to delaminate from the substrate) Low current efficiency	[35]

Table 3.7 Overview of sulfite-based electrolytes: composition, process parameters, and applications

Application	X-ray masks	Microdevices	Microbumps
Metal salt (mol/L)	0.126	0.061–0.126	0.05
Complexing agent for metal cation	Sulfite	Sulfite	Sulfite Sulfate Chloride
Other additives	EDTA; 1,2-Ethylendiamin	EDTA 1,2-Ethylendiamin Brightener (also As(III))	EDTA As(III)
pH	7	7–9.5	9.0±0.2
Temperature (°C)	55 ± 2	28–70	
Current density (A/dm^2)	0.1–0.2	0.1–0.6	0.25–0.3
References	[32]	[32]	[15]

3.3.1.11 Nickel Alloys

The rapid development of the field of microsystems has generated new applications, which in turn require materials to meet new performance demands. In this regard, electroplated alloy materials can cover a wide spectrum of different properties depending on their composition. Plating of alloys is generally more complicated than plating of single-element metals because multiple metal reductions must occur in parallel. These reduction reactions often interact with each other, creating complex electrochemical processes.

Plating of Ni alloys in general is described in [9, 12, 36]. In [37] the effect of pulse plating on the deposit quality of alloys is described in detail. In microfabrication, nickel–iron (Ni–Fe) alloys are well known for their versatility, making them suitable for micromechanical and magnetic applications [38–44]. Also some investigations on the electroplating of Ni–Co–Fe for magnetic MEMS application are described in the literature [45–47].

Ni alloys feature a number of superior material properties compared to pure nickel. Such alloys usually exhibit increased hardness and lower brittleness and can, most notably, withstand static and dynamic strains. The latter enables an improved fatigue resistance which is an important characteristic concerning the production of movable parts such as micro gear wheels or switching devices. Moreover, magnetic properties of Ni–Fe alloys are characterized by a lower coercivity and much higher permeability compared to nickel.

Independent of specific application requirements, uniform alloy composition is a common requirement for reproducible material properties. Hardness and thus wear/corrosion resistance, residual stresses, ductility, porosity, and surface roughness, as well as magnetic properties are important factors that determine the device durability. Those properties are dictated by a number of variables during the electrochemical process, such as Ni:Fe ion ratio of electrolyte, additives, bulk pH-value, temperature, agitation, and current waveform.

In the past, reports on various approaches have delved into the control of certain layer properties of microdevices including material composition and metallurgical structure by varying electrolyte formulation and process parameters [44, 48–53]. In recent years, the influence of pulse plating on material properties and composition of Ni–Fe alloys for MEMS have been investigated [e.g., 47, 54–57].

In an acid Ni–Fe electrolyte the metal ions are usually provided by chloride or sulphate metal salts whereby a soluble nickel anode can act as an additional nickel ion source. The organic boric acid is an important additive as it prevents the hydrogen evolution at the cathode by buffering the pH and thus increases cathodic current efficiency and enables a wider current density range. In addition to acting as a buffer agent, the boric acid may also alter the composition of the Ni–Fe alloy. Another additive is citrate, which is a complexing agent for the Fe^{2+} ions and thus hinders the formation of unwanted Fe^{3+} ions. Citrate also shifts the Fe overpotential to more negative values due to the higher stability of complexed ions. Furthermore, a wetting agent such as sodium dodecylsulfate (SDS) can be added to ensure complete

UNCORRECTED PROOF

wetting of the cathode. Saccharin is effective as a stress reliever. The decrease in the residual stress can be obtained by increasing the saccharin content of an electrolyte.

In Table 3.8 some recipes for sulfate-based electrolytes are summarized. The electroplated deposits have an iron content of 10–35%. In the maintenance of Ni–Fe electrolytes, control of the concentration of the electrolyte composition is crucial. To prevent Fe^{3+} formation, the electrolyte should be percolated by an inert gas (nitrogen or argon). Another option to keep oxygen out is to maintain a protective layer of argon gas over the electrolyte.

Table 3.8 Some sulfate and sulfate-chloride based Ni–Fe electrolytes for microfabrication

	Sulfate-based		Sulfate-chloride based
Bath constituents and parameters	1	2	3
Nickel sulfate ($NiSO_4 \cdot 7H_2O$) (g/L)	50	45	
Nickel chloride ($NiCl_2 \cdot 6H_2O$) (g/L)			44
Iron sulfate ($FeSO_4 \cdot 7H_2O$) (g/L)	3	3.5	
Iron chloride ($FeCl_2 \cdot 6H_2O$) (g/L)			1.1
Boric acid (H_3BO_3) (g/L)	25	25	35
Saccharin($C_7H_4NNaO_3S.2H_2O$) (g/L)	1	1	1.5
Sodium citrate ($Na_3(C_6H_5O_7) \cdot 2H_2O$) (g/L)	28		
Sodium-dodecyl-sulfate ($NaC_{12}H_{25}SO_4$) (g/L)	0.5	0.5	0.4
pH	3.5	2.8	2.5
Temperature (°C)	50	50	35
Current density (A/dm^2)	2–4	0.5	0.6
Thickness of electroplated micro structures reported (µm)	500	80	2
References	[57]	[50]	[48, 49]

3.3.2 Electroless Plating

Electroless plating requires no external source of electrical current. The term "electroless plating" is generally used to describe three fundamentally different plating processes: galvanic displacement, substrate-catalyzed processes, and autocatalytic processes. Galvanic displacement induces electron exchange on the surface of the substrate in the electrolyte, resulting in the reduction of metal ions. The substrate-catalyzed process modifies the surface to make it more reactive for oxidation and reduction. In these first two processes, the plating reaction should cease when the substrate is covered completely with metal, whereas in the autocatalytic process a metal salt and a reducing agent in an aqueous solution react continuously in the presence of a catalyst, making this technique more suitable for thick layers of metal. Chemical reducing agents often employed are hydrazine, sodium hypophosphite, sodium borohydride, amine boranes, titanium chloride, and formaldehyde.

A general reaction in electroless plating is described as:

$$M^{z+}\ (\text{Metal ion}) + z\,e^{-}(\text{suppliex by reducing agent}) \xrightarrow{\text{catalytic surface}} M\ (\text{deposit})$$

This reaction can occur only on a catalytic surface; once deposition is initiated, the deposited metal must be self-catalytic to enable continued deposition.

Not all metals show self-catalytic functionality, and thus the kinds of metal for electroless plating are limited. Since Brenner and Riddell [58] first reported nickel electroless plating in an autocatalytic sense, electroless plating has continuously advanced, and now many useful metals are plated electrolessly. Those materials include nickel, cobalt, palladium, platinum, copper, gold, silver, and certain alloys. Various bath chemistries are available for each metal, each with different metal salts, reducing agents, and complexing agents. Some of the electroless plating baths and conditions for nickel, copper, and gold are introduced in the following sections.

Electroless plating is useful for metal deposition on nonconducting surfaces such as polymers or inorganic layers. However, because the physical and chemical properties of metals and polymeric or inorganic materials are quite different, the adhesion between two materials is often very poor and the plated metals tend to peel off. To improve adhesion and to increase the number of catalytic sites on the surface, a sample needs to go through surface treatment by physical/chemical etching processes and surface catalysis prior to immersing in the electroless plating bath.

A brief procedure flow is shown in Fig. 3.13. The surface modification includes nanoscopic surface roughing using chemical wet/dry etching (e.g., reactive ion etching) to increase the interfacial surface area for better adhesion. Then the sample is catalyzed. One popular catalyzing procedure uses a surface treatment with mechanically compliant tin, followed by the major catalytic compound palladium. In order to provide uniform catalytic sites on the surface and provide a kinetic energy during the metal reduction on the surface, both the catalysis and electroless plating steps are performed in ultrasonic environment [59, 60].

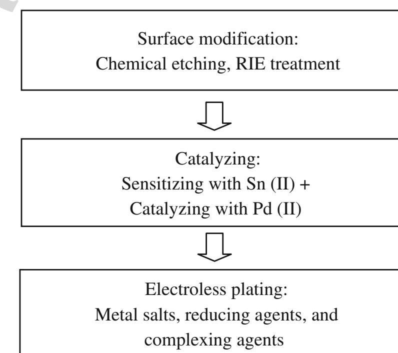

Fig. 3.13 An example of a procedure for electroless plating

UNCORRECTED PROOF

3.3.2.1 Nickel

Electroless nickel plating is one of the most popular catalytic electroless processes in use today. It is commonly used in engineering coating applications for wear resistance, hardness, and corrosion protection. It is also used in the electronics industry on PCBs as a coating with an overlay of gold to prevent corrosion. The concept and basic composition has not changed much since the inception of the process [58]. The electroless nickel plating bath consists of a source of nickel ions (salts), a reducing agent, complexing agents, and some additives.

Although many nickel salts such as nickel sulfate, nickel chloride, and nickel acetate are available, nickel sulfate is preferred because of its low corrosiveness and low cost. To enhance chemical reduction of nickel at the cathode, a reducing agent is used such as sodium hypophosphite (NaH_2PO_2 H_2O), sodium borohydride ($NaBH_4$), and dimethylamine borane (DMAB). Complexing agents are used for exerting a buffering action to prevent the pH change, preventing the precipitation of nickel salts, and enhancing stable metal reduction. Note that because there are several agents inserted in the bath, nickel from electroless plating is not usually pure but contains other components such as phosphorus or boron.

Table 3.9 shows some bath compositions for electroless nickel deposition with hypophosphite reducing agent (columns 1–4), borohydride reducing agent (columns 5–6), and dimethylamine borane reducing agent (columns 7–8) [61].

A step-by-step procedure for nickel electroless plating with a hypophosphite reducing agent is given below [9, 62], which essentially follows the recipe of Table 3.9 (column 1) except for the amount of hydroxyacetic acid of 30.9 g/L and the process temperature of 65°C. With this recipe, a deposition rate of approximately 70 nm/min (4.2 µm/h) is obtained on a printed circuit board and a Si substrate. The equipment necessary for electroless nickel plating is shown in Fig. 3.14, consisting of an Sn sensitizing bath, a Pd activation bath, an electroless nickel bath, and an ultrasonic bath.

Bath Preparation

1. Mix 10 g of $SnCl_2$ and 10 g of HCl. Take 0.375 mL of the solution and mix it with 120 mL of deionized water to prepare the Sn(II) solution.
2. Mix 10 g of Pd and 10 g of HCl. Take 0.5 mL of the solution and mix it with 100 mL of deionized water to prepare the Pd(II) solution.
3. Measure 129.62 g $NiCl_2$, 105.97 g $NaH_2PO_2{\cdot}H_2O$, and 61.8 g $HOCH_2COOH$ into a 1 L beaker. Fill the beaker with deionized water to 1 L. Mix using a motorized mechanical propeller for at least 2 h. (Note that a magnetic stirring bar is not recommended because the bath contains ferromagnetic Ni.) This stock solution can be stored for a month or two without noticeable degradation.
4. Add NH_4OH to obtain a pH level of 4–6. Mix well for 2 h in a similar way to that described above. This pH adjustment should be performed immediately before performing electroless plating.

Table 3.9 Example baths for electroless nickel deposition using various hypophosphite reducing agents

Bath constituents and parameters	Hypophosphite reducing agent				Borohydride reducing agent		Dimethylamine borane reducing agent	
	1	2	3	4	5	6	7	8
Nickel chloride ($NiCl_2{\cdot}6H_2O$) (g/L)	30	30	30		20	24	170	
Nickel sulfate ($NiSO_4{\cdot}6H_2O$) (g/L)				25				30
Sodium hypophosphite ($NaH_2PO_2{\cdot}H_2O$) (g/L)	10	10	10	25				
Hydroxyacetic acid ($HOCH_2COOH$) (g/L)	35							
Sodium citrate ($Na_3C_6H_5O_7{\cdot}2H_2O$) (g/L)		12.6	84					
Sodium acetate ($NaC_2H_3O_2$) (g/L)		5						
Sodium borohydride ($NaBH_4$) (g/L)					0.67	0.4		
Ethylenediamine ($C_2H_4(NH_2)_2$) (g/L)					44			
Sodium hydroxide (NaOH) (g/L)					40			
Ammonium hydroxide (NH_4OH, 28% NH_3) (mL/L)						120		
Dimethylamine borane ($(CH_3)_2NHBH_3$) (g/L)							37	3.5
Malonic acid ($C_3H_2O_4Na_2$, disodium salt) (g/L)								34
Ammonium chloride (NH_4Cl) (g/L)			50					
Boric acid (H_3BO) (g/L)							25	
Sodium pyrophosphate ($Na_4P_2O_7{\cdot}10H_2O$) (g/L)				50				
Base for neutralizing	NaOH	NaOH	NH_4OH	NH_4OH	NaOH	NH_4OH	NaOH	NH_4OH
pH	4–6	4–6	8–10	10–11	11	11	4.25	5.5
Temperature (°C)	90–100	90–100	95	70	97	60	18	77
Deposition rate (µm/h)	15	7	6.5	15	8.8	1.3	2.3	21
References	[62]	[63]	[58]	[64]	[65]	[65]	[66]	[67]

UNCORRECTED PROOF

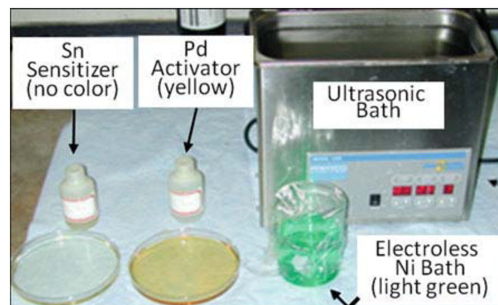

Fig. 3.14 Preparation of electroless nickel plating

This figure will be printed in b/w

Electroless Nickel Plating Procedure

1. Rinse a substrate in acetone, then methanol, then deionized water, and then sensitize it in the Sn(II) solution for 2 min.
2. Rinse the sample in deionized water for 30 s.
3. Catalyze the sample in the prepared Pd(II) solution for 2 min.
4. Rinse the sample in deionized water for 30 s.
5. Submerge the sample in the prepared electroplating bath at 65°C in an ultrasonic environment.

AQ2

Table 3.10 Ingredients of electroless nickel bath with hypophosphite reducing agent [9]

Bath constituents and parameters	Molarity (mol)	Molecular weight	Mass (g/L)
Nickel chloride ($NiCl_2{\cdot}6H_2O$)	0.23	129.62	30
Sodium hypophosphate ($NaH_2PO_2{\cdot}H_2O$)	0.09	105.97	10
Hydroxyacetic acid ($HOCH_2COOH$)	0.5	61.8	30.90
pH	4–6 (using NH_4OH or NaOH for adjustment)		
Temperature	65°C		

3.3.2.2 Copper

Some electroless copper plating recipes use formaldehyde or its derivatives as a reducing agent. However, such plating baths produce toxic formaldehyde vapor during the process and require high pH (~12.5). An alternative bath uses hypophosphite as the reducing agent. Table 3.11 shows some bath compositions for electroless copper deposition with formaldehyde reducing agent (columns 1–3) and hypophosphite reducing agent (column 4) [61, 68].

UNCORRECTED PROOF

Table 3.11 Example baths for electroless copper deposition using formaldehyde reducing agent and hypophosphite reducing agent

	Formaldehyde reducing agent			Hypophosphite reducing agent
Bath constituents and parameters	1	2	3	4
Copper sulfate ($CuSO_4{\cdot}5H_2O$) (g/L)	3.6	30	10	3.83
Nickel sulfate ($NiSO_4{\cdot}6H_2O$) (g/L)				0.53
Boric acid (H_3BO_3) (g/L)				30.9
Sodium hypophosphite ($NaH_2PO_2{\cdot}H_2O$) (g/L)				28.6
Sodium potassium tartrate ($KNaC_4H_4O_6{\cdot}4H_2O$) (g/L)	25	99		
Sodium hydroxide (NaOH) (g/L)	3.8	50	10	
Sodium carbonate (Na_2CO_3) (g/L)		32		
Formaldehyde (HCOOH (37%)) (g/L)	10	29	20.3	
Sodium citrate ($Na_3C_6H_5O_7{\cdot}2H_2O$) (g/L)				15.3
Methyldichlorosilane (CH_3Cl_2SiH) (g/L)			0.25	
Ethylenediaminetetraacetic acid (EDTA) tetrasodium (N,N′-1,2-Ethanediylbis[*N*-(carboxymethyl)glycene] tetrasodium) (g/L)			20	
Temperature (°C)	22	25	63	65
Deposition rate (µm/h)	0.5	2.5	6.3	8.5
References	[69]	[70]	[71]	[68]

The hypophosphite reduced electroless copper plating has advantages including bath stability, no toxic gas generation, and operation in a lower pH environment. However, because the deposited copper cannot catalyze the oxidation of hypophosphite, the bath needs a small amount of nickel for continuous plating and boric acid for a high plating rate, resulting in impure copper deposition.

A step-by-step procedure for copper electroless plating with a hypophosphite reducing agent [68] is given below as an example.

Bath Preparation

1. Mix 10 g of $SnCl_2$ and 10 g of HCl. Take 0.375 mL of the solution and mix it with 120 mL of deionized water to prepare the Sn(II) solution.
2. Mix 10 g of Pd and 10 g of HCl. Take 0.5 mL of the solution and mix it with 100 mL of deionized water to prepare the Pd(II) solution.
3. Mix the electroless copper plating bath with hypophosphite reducing agent following Table 3.11 (column 4).
4. Adjust the pH with either KOH or NaOH pellets to the desired pH level (Here it is 9–9.5).

Note that all ingredients are mixed and dissolved in water together. The mixture after step 3 can have a shelf life of about a month, but the mixture after step 4 tends

UNCORRECTED PROOF

to plate a thin copper layer on the container wall in a few days. The pH adjustment should be done right before electroless plating is performed. The solution should have a clean blue color.

Electroless Copper Plating Procedure

1. Rinse substrate in acetone, then methanol, and then deionized water, and then sensitize it in the prepared Sn(II) solution for 2 min.
2. Rinse the substrate in deionized water for 30 s.
3. Catalyze the substrate in the prepared Pd(II) solution for 2 min.
4. Rinse the substrate in deionized water for 30 s.
5. Submerge the substrate in the prepared electroless plating bath.

3.3.2.3 Gold

Because of its high chemical stability and mechanical ductility, gold becomes an indispensable material in the electronics industry. Despite its importance, electroless gold plating [29] has been underdeveloped compared with electroless nickel or copper. Useful electroless gold plating using borohydride or amine borane as the reducing agent has been reported [72, 73]. A typical bath composition is shown in Table 3.12.

Table 3.12 Ingredients of electroless gold bath with borohydride reducing agent [73]

Bath constituents and parameters	Molarity (mol)	Molecular weight	Mass (g/L)
Potassium gold cyanide ($KAu(CN)_2$)	0.02	290	5.8
Potassium cyanide (KCN)	0.2	65	13
Potassium hydroxide (KOH)	0.2	56	11.2
Potassium borohydride (KBH_4)	0.4	54	21.6
Temperature	75°C		
Deposition rate	0.7–3.5 µm/h (with stirring)		

Bath Preparation (2.5× Concentration) [67]

1. Dissolve 28 g KOH and 32.5 g KCN in about 500 mL of deionized water.
2. Add 54 g KBH_4 and stir until dissolution.
3. Dissolve 14.4 g $KAu(CN)_2$ in about 250 mL deionized water.
4. Mix the above two solutions, and dilute to 1 L.
5. Filter through Whatman 41 filter paper or equivalent.
6. Dilute 1 volume of this solution with 1.5 volumes of deionized water to make a 2.5× bath.

UNCORRECTED PROOF

3.3.3 Comparison of Electroplating and Electroless Plating

Ni, Cu, and Au microstructures can all be fabricated by electroplating or electroless plating. Compared to electroplating, electroless plating contains the following characteristics and advantages [61].

1. No power supply and electrical contact is necessary.
2. Deposition may occur on a nonconducting surface.
3. More uniform deposition can be formed on three-dimensional geometry without electric field influence.
4. Deposits are often less porous.

There are disadvantages of electroless plating too. Often the electroless baths require higher temperatures and have a relatively short lifetime. Electroless plating is also prone to poor adhesion. Care should be taken when storing electroless plating baths. A container made of plastic or glass is often found to be covered with electroless plated metal after being stored on the shelf for a while. Also, for electroless plating, the deposition rate is relatively slow, and metal layers thicker than a few micrometers are not recommended. In addition, electroless plating metal in selected regions can sometimes be quite challenging. For example, selective deposition on a metal surface is fairly easy, but selective coating a polymer on SiO_2 is not very effective (the bath will likely deposit on both the polymer and SiO_2 surfaces).

Costs of electroplating and electroless plating are fairly similar. The electroless plating process requires a chemical reducing agent for metal ions to be converted into the elemental conformation, therefore it is considered as a more expensive process from the material cost point of view. However, this chemical cost is offset by the advantage of not requiring equipment such as power supplies or switching circuits for advanced current control.

There are clearly pros and cons associated with both electroplating and electroless plating. In situations where either electroplating or electroless plating could theoretically be used, the decision for one or the other is often dependent on many process integration issues. In general, electroless plating can be considered as a complement to electroplating rather than a “competitor.”

3.4 LIGA and UV-LIGA Processes

One of the most distinctive MEMS processes is the construction of thick and high-aspect-ratio three-dimensional (3-D) microstructures. High aspect ratio is modestly defined as a height to width ratio of 2 to 1 or greater. Fabrication of these structures often relies on X-ray or UV lithography of thick polymer layers.[4] The patterned

[4] See Chapter 9 for more information on lithography.

UNCORRECTED PROOF

1486 polymeric structures can be used directly as a MEMS device or used as a mold for
1487 metal electrodeposition. In this section, two fabrication approaches for achieving
1488 high-aspect-ratio 3-D electroformed metallic structures are described: one with X-
1489 ray lithography (LIGA), and the other with UV lithography (UV-LIGA or LIGA-
1490 Like).[5]
1491
1492
1493 ### 3.4.1 Process Explanation
1494
1495 Both LIGA and UV-LIGA processes share common fabrication steps except for the
1496 initial step of polymeric mold fabrication. A general fabrication procedure for both
1497 processes is described in this section.
1498 Because these are surface micromachining processes, there is no strict crite-
1499 rion for substrate selection. A variety of substrates such as Si, glass, ceramic, and
1500 printed wiring board are available, however, an oxidized Si substrate is used as an
1501 example here (Fig. 3.15). An electrical seed layer typically consisting of Ti/Cu or
1502 Cr/Cu is deposited on the substrate using either sputtering or evaporation. Cu does
1503
1504

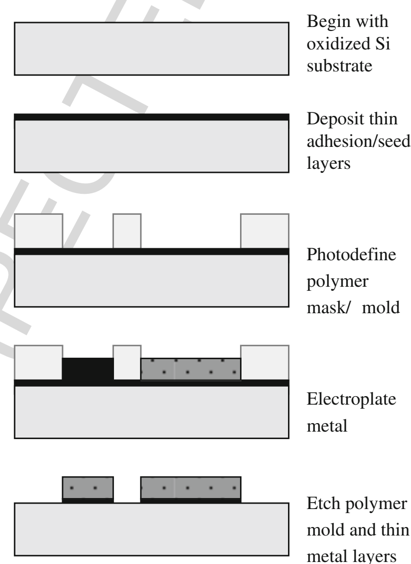

Fig. 3.15 Basic electroplating process to form single-layer metal structures

[5]The German acronym "LIGA" refers to a three-step process: X-ray-*Li*thography, Electroplating (german: *Galvanik*), Polymer Replication (German: *Abformung*). Nowadays, "LIGA" is commonly used in reference to the two-step process of lithography and electroplating (excluding the polymer replication step).

UNCORRECTED PROOF

SPB-140376 Chapter ID 3 October 29, 2010 Time: 08:22pm Proof 1

1531 not stick well to most substrates so Ti or Cr is employed as an adhesion layer
1532 (see Section 3.5.1). Typical thicknesses of Ti (or Cr) and Cu are 10–30 nm and
1533 100–300 nm, respectively. After the seed layer deposition, a thick polymer layer
1534 is coated, soft-baked, and lithographically patterned to form a micromold for a
1535 subsequent electroplating. LIGA typically uses polymethylmethacrylate (PMMA)
1536 or SU-8 (an epoxy-based polymer) for X-ray lithography, whereas UV-LIGA uses
1537 various UV-sensitive photoresists including DNQ-novolak-based photoresist, SU-8,
1538 polyimide, and others.
1539 With the photoresist mold in place, the substrate is then electroplated. The elec-
1540 troplated metal fills the mold confined by the sidewalls. Usually the electroplating
1541 is stopped before it reaches the top of the mold. But sometimes it is electroplated
1542 over the mold to form "mushroom"-type structures for some applications. After
1543 electroplating, the polymer mold is removed using a solvent and/or plasma etching.
1544 The electroplated structures are still electrically connected to each other through the
1545 seed layer. The Cu and Ti seed layers are then sequentially time etched to isolate the
1546 electroplated structures electrically and complete the process.
1547 With the introduction in the 1990s of UV photopatternable high-aspect-ratio
1548 polymers such as SU-8, high-quality sidewall and high-aspect-ratio molds could
1549 be fabricated using UV lithography, as compared to X-ray lithography. The electro-
1550 forming process using UV-patterned molds and subsequent electroplating has been
1551 called UV-LIGA, LIGA-like, or often "poor man's LIGA."
1552 The UV-LIGA process does not provide the extreme aspect ratios possible with
1553 X-ray LIGA, but is sufficiently suitable for many applications. A good guideline
1554 is that an aspect ratio of 6:1 can be fabricated by UV-LIGA. It is also restricted
1555 to a maximum resist height of 800 μm or so. Also submicron pattern dimensions
1556 may not be effectively produced because of the wavelength of the UV source, for
1557 example, i-line ($\lambda = 365$ nm). However, in addition to low cost in equipment, the
1558 process has other advantages such as batch processability, manufacturability, and
1559 relative simplicity, providing an affordable system set for laboratory and industrial
1560 usage.
1561
1562
1563
1564 ### 3.4.2 Electroplating in LIGA and UV-LIGA Microstructures
1565
1566 The height and surface profile of high-aspect-ratio electrodeposited metal structures
1567 and the homogeneity of their thickness distribution are influenced by various factors,
1568 which can interfere with each other. The main factors and important effects are
1569 explained in this section.
1570 The deposition rate is proportional to the current density. Therefore a higher cur-
1571 rent density results in a thicker deposit. The distribution of the current density is
1572 associated with the distribution of the electric field lines (primary current distribu-
1573 tion). Because the metal surface is highly conductive, the field lines are normal to
1574 the electrode surface. If the anode has a larger area than the cathode, the field line
1575 density and current density are higher at the edge of the substrate, which causes a

UNCORRECTED PROOF

thicker deposit at the edge of the substrate ("macro bathtub effect"). If the cathode surface is patterned with resist structures, the electric field lines bend, and a current concentration occurs at the edge of the structures [74, 75]. Therefore the electroplated layer is usually thicker near the edges of the electroplated features ("micro bathtub effect") and sometimes higher in narrow structures than in wide structures, as shown in Fig. 3.16.

Another consideration for electroplating in high-aspect-ratio features is that the transport mechanism of the metal ions depends on feature size and depth. As a result, the electroplating rate may vary during the plating process [76]. Figure 3.17 shows three different states that occur in filling a mold structure by electroplating. At the beginning of the deposition, the process is highly diffusion limited. As the plated layer grows and the trenches begin to fill, the diffusion limitations begin to wane. At an intermediate filling, the penetration range of the convection is reached. This depends on the lateral size of the structure itself. In the case of structures with sufficiently wide lateral dimensions, the flow velocity in the plating bath reduces the extension of the diffusion layer, as described in Section 3.3.1.2. Very high-aspect-ratio structures therefore show a reduced plating rate in the beginning of plating. In this case, the electroplated layer would be thinner in narrow structures, as compared to wider structures.

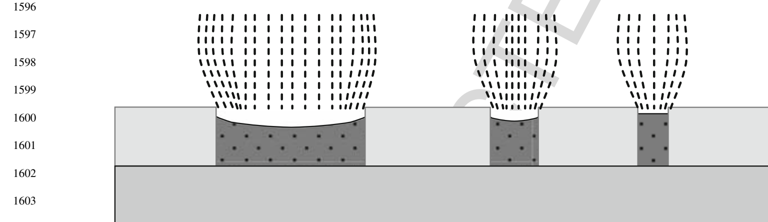

Fig. 3.16 Schematic of electrical field line distribution using resist-patterned substrates. The field line density is higher within narrow structures and at the edge of wide structures, which affects the height and surface profile of the electroplated microstructures

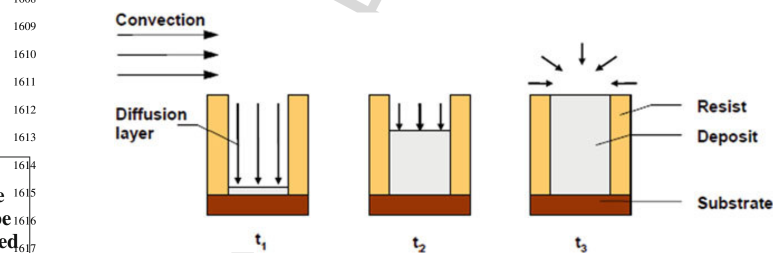

This figure will be printed in b/w

Fig. 3.17 Schematic of the diminishing influence of diffusion during metal growth. The diffusion layer thickness depends on process progress and on the penetration range of convection. At t_3, the deposition rate is improved due to spherical diffusion

All these effects cause inhomogeneous deposition rates over the substrate as well as within the features. To minimize these unwanted effects and improve the plating uniformity, some rules are given in the following.

1) Use a shield or a wafer holder to homogenize the electrical field at the macroscopic scale.
2) Use dummy plating areas over the whole substrate to promote a homogenous current distribution.
3) Use microstructured dummy areas that surround the functional features.
4) Use moderate flow to get similar heights of diffusion layers.
5) Use moderate current density to avoid insufficient supply of ions at the bottom of the microstructure.
6) Limit the deposition height to be about 2/3 of the mold height (see Fig. 3.17 for t_2).

More rules for LIGA design can be found in [77].

To show the potential of the LIGA techniques, one example is given. Figure 3.18 shows (a) a SU-8 resist mold and (b) the replicated Ni–Fe structure. The electroplating produces the exact negative of the structural details and the sidewall roughness of the resist mold. In Fig. 3.19 a commercially available micro gear system is shown. Crucial features for this application are the high aspect ratio in combination with the parallel sidewalls of the resist structure, which is typical for LIGA. Other applications of LIGA are described in [78, 79].

3.4.3 Multilevel Metal Structures

Often multiple metal levels and vias are necessary to enable complex wiring interconnections or complex mechanical microstructures. Multilevel fabrication can be achieved by extending the previously described process (see Section 3.4.1) using multiple masking and electroplating steps. For wire connections, an interlayer dielectric material must be selected to electrically insulate the metal layers from each other to avoid unexpected short circuits. Considering that the top surface of the first metal layer may be fairly rough (typical of many electroplated metals), the dielectric must be able to conformally and completely coat the top and side surfaces of the lower metal layer. Even the smallest pinhole defect in the interlayer dielectric can cause the electrical insulation to fail. Commonly used interlayer dielectric materials include PECVD or sputtered oxide/nitride, spin-on glass, or a chemically stable spin-coated polymer such as polyimide or SU-8. The intended temperature of operation must also be considered, because polymer dielectrics may not be suitable at a 100°C or more.

A fabrication process for achieving a two-layer metal structure is shown in Fig. 3.20. The process begins by depositing the first metal layer as described in Fig. 3.15. The interlayer dielectric is deposited and vias are opened to provide

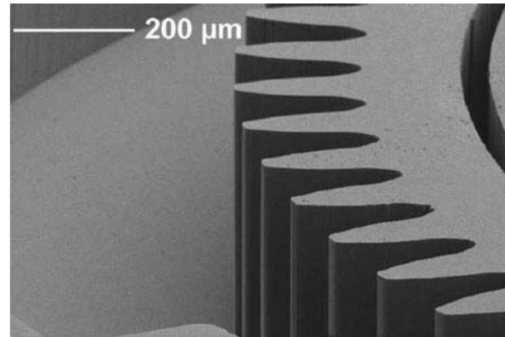

(a)

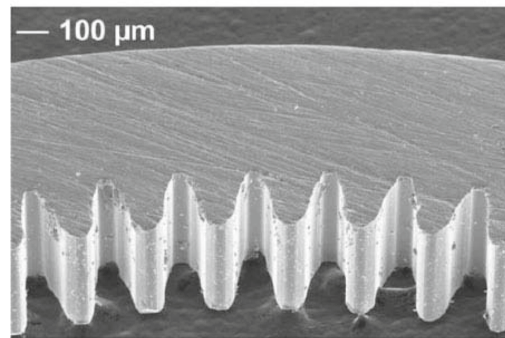

(b)

Fig. 3.18 SEM micrograph of high-aspect-ratio microstructures: (**a**) SU-8 resist mold; (**b**) electroplated Ni–Fe [57] (Reprinted with permission. Copyright 2008 Springer Europe)

interconnects between the two metal layers. For many films, this step requires the patterning of a photoresist mask and a subsequent etch. In contrast, the use of a photosensitive polymer dielectric offers the opportunity for simple one-step photodefinition.

After the interlayer dielectric is formed, a new adhesion/seed layer is required, because a conductive electrical surface is needed for electroplating. In order to provide sufficient step-coverage over the topography created by the first metal layer, sputtering is the preferred method. It should be noted that adhesion of the metal to a polymer interlayer dielectric can be quite low. If necessary, adhesion promoters may be used to improve adhesion of the metal (see Section 3.5.1).

After the seed layer deposition, a polymer mold is photodefined to create the pattern for the second metal layer, and the metal is subsequently electrodeposited to the desired thickness. Afterwards, the polymer mold and thin metal layers are etched away. If necessary a passivation layer can be deposited on top of the second metal layer for protection from the environment. Also with the right selection of materials,

SPB-140376 Chapter ID 3 October 29, 2010 Time: 08:22pm Proof 1

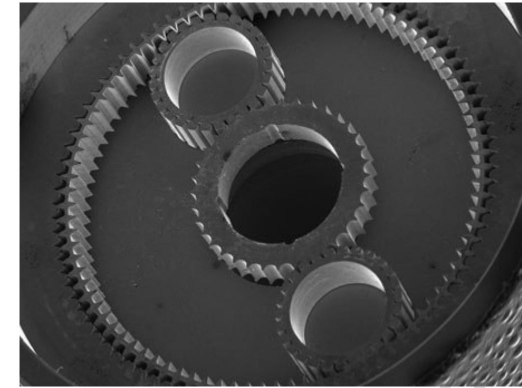

Fig. 3.19 Ni–Fe microplanetary gear system; structure height = axial length : 1 mm, diameter 8 mm (Reprinted with Permission. Copyright 2009 Micromotion GmbH, Germany)

the interlayer dielectric can be selectively etched away to create "free-standing" bridge segments that are isolated by air [80–82].

In addition to the planar metal layers, some MEMS devices creatively employ high-aspect-ratio vertical via structures for mechanical or electrical functionality. For example, metal vias are used for vertical interconnects in MEMS packaging applications [83] and for electrical passive components in RF MEMS [84]. Fabrication of vias with high aspect ratios is often desired, and various methods for achieving such structures are shown in Fig. 3.21.

The different characteristics of these approaches are summarized in Table 3.13 and described as follows. First is the damascene process, used extensively in silicon VLSI processing [85]. In damascene, an oxide mold is used, and conformal seed layers are sputtered, followed by copper electrodeposition. Excess copper protruding from the molds is removed by chemical mechanical polishing (CMP),[6] leaving copper only in the via or trench. The interdielectric oxide layers bounding the copper are intended to remain at the end of the process, serving as an electrical insulator and mechanical supporting layer for the subsequent processes.

For 3-D polymeric-mold-based processes such as LIGA or UV-LIGA, CMP may damage the softer polymer mold material resulting in uneven surface morphology. To avoid polishing steps, several alternatives have been explored. The plate-through-mold approach uses seed layers deposited before the molds. The plating time is proportional to the depth of the mold, and the mold often must be removed after the plating, which lengthens the process time further. Moreover, removal of some polymeric molds such as polyimide or SU-8 often relies on expensive (and relatively slow) dry etching processes.

[6] See Chapter 13 (specifically Section 13.7) for more information on CMP.

UNCORRECTED PROOF

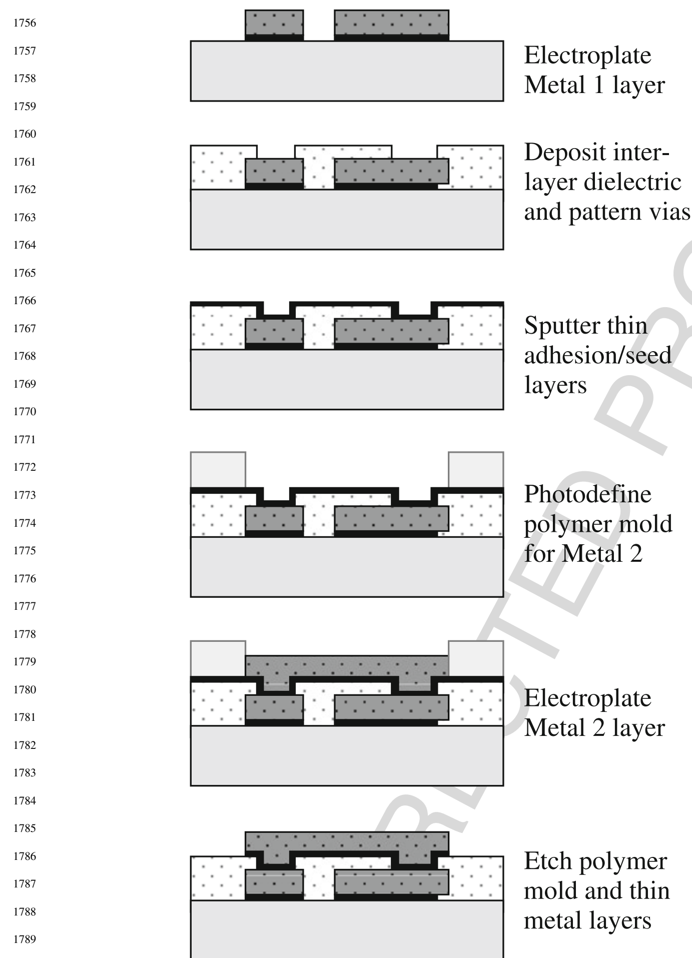

Fig. 3.20 Electroplating process to form multilayer conductive layers

Another approach – a wet etch back process – has also been used for high-aspect-ratio via connections with polymer molds [86]. This process is similar to damascene, except that a wet chemical etch is used to etch back protruding copper, as opposed to CMP. Although suitable for polymer molds, planarity is problematic.

An embedded conductor fabrication (as previously described in Fig. 3.20) uses mold formation and a combination of two simultaneous plating processes: a conformal plating process through nonremovable lower via mold and a conventional

UNCORRECTED PROOF

SPB-140376 Chapter ID 3 October 29, 2010 Time: 08:22pm Proof 1

This figure will be printed in b/w

Fig. 3.21 Fabrication process comparison for one via and one upper conducting layer configuration: (**a**) damascene process; (**b**) conventional plate-through-mold process; (**c**) conformal plating process with etch back; (**d**) conformal plating without etch back [84] (Reprinted with permission. Copyright 2005 IOP)

plate-through-mold process through a removable upper conductor mold [84]. The vias are embedded in the mold from which they are formed: the mold is not removed after the structures are completed. This eliminates a long etching step for the mold removal, which simplifies and shortens the process. Also, the conformal plating makes the via fill time independent of the via height. At the end of the process, the conductors are embedded in the mold, resulting in good mechanical strength for subsequent process or packaging steps. The low-temperature polymeric process also facilitates post-CMOS compatibility if necessary.

UNCORRECTED PROOF

Table 3.13 Various processes for multilayer conductor layers with vias [84]

	Damascene	Conventional plate-through-mold process	Conformal plating process with etch back	Conformal plating process without etch back
Mold material	Oxide (ceramic)	Polymer (organic)	Polymer (organic)	Polymer (organic)
Mold removal	No	Yes	No	No
Metal deposition time	Short	Long	Short	Short
Number of plating per two layers	2	2	2	1
Excess metal removal	Polishing(CMP)	No	Chemical etching	No
Mold erosion or metal dishing	Susceptible during CMP	N/A	Metal dishing during etch-back	N/A
Metal source usage	Noneconomical	Economical	Noneconomical	Economical
Device packaging	Injection molding	Polymer or cavity packaging	Injection molding	Injection molding
Applications	IC interconnect	MEMS actuator, RF passives, interconnect, power devices	MEMS interconnect, RF passives, power devices	MEMS interconnect, RF passives, power devices
References	[85]	[80]	[86]	[84]

Reprinted with permission. Copyright 2005 IOP

3.5 Materials Properties and Process Selection Guidelines for Metals

This section provides general guidelines for the selection of metals for use in MEMS. It also provides relevant material properties and application issues relating to adhesion, electrical, mechanical, thermal, and magnetic aspects.

3.5.1 Adhesion

Regardless of the intended functional application, adhesion of any metal to a particular substrate is critical to ensure successful microfabrication and long-term reliability. Adhesion depends on many factors, including type of substrate, roughness of the substrate, deposition methods, thickness of the film, and so on. The adhesion is determined by the interfacial energies of the interface, which may be metal–metal, metal–dielectric, or metal–polymer. Delamination occurs when the intrinsic and extrinsic stress in the deposited metal films overcomes the interfacial energy. Generally, cracking is caused by tensile stress, and peeloff by compressive stress.

Intrinsic stress is the result of crystallographic defects in the film, and extrinsic stress is due to the thermal expansion mismatch between the film and substrate [87]. For most MEMS applications, the extrinsic stress plays a major role. However, intrinsic stress can also be problematic. For example, stress accumulates with increasingly thick electroplated films, so this stress often limits how thick an electrodeposited layer may become.

Table 3.14 qualitatively summarizes the adhesion of various metals to different materials. Many metals, especially noble metals, do not adhere very well to common MEMS substrates such as Si, SiO_2, or glass. Often, however, thin layers of interfacial materials can be used to improve adhesion. The most widely used adhesion enhancing layers are Ti and Cr (as well as Ta and W) with thickness of 5–20 nm, usually sputtered or evaporated.

The reason for this enhancement is as follows [91]. These adhesion-promoting metals all readily oxidize, in contrast to noble metals such as Au, Ag, and Pt. Thus,

Table 3.14 Qualitative adhesion of thin film metals to different substrates

	Si [87]	SiO_2 [87]	Polyimide [88, 89]	PDMS [90]
Al	Moderate	Good	Moderate	–
Au	Moderate	Poor	Poor	Poor
Cr	Good	Good	Good	Good
Cu	Moderate	Poor	Poor	Poor
Ni	Moderate	Good	Poor	–
Pt	Moderate	Good	–	Poor
Ta	Good	–	Good	–
Ti	Good	Good	Good	Good

UNCORRECTED PROOF

when an adhesion-promoting metal is deposited onto a substrate such as SiO_2, glass, or even a "clean" Si wafer with just monolayers of native oxide, chemical bonding occurs between the metal and the substrate by partial oxidation of a very thin interfacial layer of the metal. That oxide formation results in covalent bonding between the adhesion-promoting metal and the substrate. A metal deposited on top of this adhesion layer metal can interdiffuse with the adhesion-promoting metal and thus provide strong bonding of the top metal. For this mechanism to occur, the adhesion-promoting layer must not be exposed to air before depositing the second metal layer on top. If the top surface of the adhesion layer is air oxidized, it can no longer interdiffuse with the top metal, hence the bond between the two metals will be very weak and adhesion poor.

Many MEMS applications employ metals deposited on polymers. Metal–polymer interfacial issues are much more complex, with adhesion dependent on the concentration of functional groups on the polymer surface and the bond strength between the metal atoms and these functional groups [92]. The metal diffusion depth into a polymer has been found to inversely correlate with adhesion, that is, lower diffusion corresponding to stronger adhesion [89]. Other environmental and processing factors also play a role, as described below.

For polyimide, the adhesion of thin-film metals is generally good. Cu and Ni weakly bind to polyimide, Cr bonds strongly, and Al is somewhere in between [89]. In order to improve adhesion, an interfacial layer such as Ta can be used [93]. Or prior to deposition of metal, the polyimide surface can be modified by oxygen plasma, argon sputtering, or chemical etching (KOH) to enhance adhesion [88]. Note, however, metal–polyimide adhesion may deteriorate with exposure to high temperatures or high humidity [88].

PDMS has very low surface energy, so that when metals are deposited on top of it, wavelet morphology may occur on the PDMS surface [90]. This deformation may cause discontinuities or rupture of thin metal lines. Nevertheless, the adhesion of Ti and Cr on PDMS is good, so these are often used as an adhesion layer between PDMS and other metals such as Au and Pt. In addition, it is reported that the adhesion of metal with PDMS can be enhanced by plasma-treating the PDMS surface [92].

3.5.2 Electrical Properties

Metals are widely used in MEMS for electrical properties. Many pure metals are highly conductive, exhibit good adhesion to MEMS substrates, and good stability. Electrical interconnections (wires) are the most obvious and widespread electrical application for metals. Here, the most important parameter is the electrical resistivity (or inversely, conductivity). However, there are many other factors when considering selection of an appropriate metal for electrical applications. Table 3.15 summarizes some of these parameters, which are further discussed below.

The effect of skin depth must be considered for metals that will conduct high-frequency AC currents. The "skin effect" is the tendency for currents to be forced to

Table 3.15 Electrical properties of metals[a]

	Electrical resistivity (μΩ cm) [94]	Temperature coefficient of resistance (10^{-3} K^{-1}) [95]	Solderable [96]	Wire bondable [97, 98]	Self-passivating oxide [99]
Ag	1.62	3.8	Yes	Al	No
Al	2.71	3.6	Difficult	Au, Al	Yes
Au	2.26	8.3	Yes	Au, Al	–
Cr	12.6	3.0	No	No	Yes
Cu	1.71	3.9	Yes	Au[b]	No
Ni	7.12	6.9	No	No	Yes
Pt	10.7	3.9	Yes	Al	–
Ta	13.4	–	Yes	Al	Yes
Ti	39.0	–	No	No	Yes
W	5.39	4.5	No	No	–

[a]Electrical resistivity at 25°C; TCR values at 20°C
[b]Difficult, and reliability uncertain

the surface of a conductor, thus making the wire appear more resistive with increasing frequency. For this reason, increasing the cross-sectional area of a metal much beyond the skin depth does not result in lower resistance for an AC signal. The skin depths of most metals are only tens of micrometers above 1 MHz (e.g., the skin depth of Cu at 1 MHz is ~65 μm [100]). Most metals have a relative permeability of approximately unity, however, Ni and other ferromagnetic metals can have large permeabilities, leading to even smaller skin depths.

Most conductive materials also exhibit a change in resistance with temperature. The percentage resistance change per degree Celsius is referred to as the temperature coefficient of resistance (TCR) and is specified at a standard temperature. Most metals have a positive TCR, meaning that the resistance increases with temperature. The TCR is an important design consideration when metal structures are subjected to high/low temperatures or thermal cycling, especially for resistive-based sensors where unpredictable changes in interconnect resistance may affect the overall sensor performance. Metallic structures may also be specifically designed to take advantage of the TCR for sensing as a resistive temperature detector (RTD). In particular, Pt has a stable TCR over a wide temperature range, relatively high baseline resistivity, and good thermal stability, making it an ideal choice for use as an RTD.

Thermal and chemical stability are also critical to the long-term functioning of metals. Oxidation will occur on the surface of most metals in the presence of air. The impact of this oxidized layer will vary from metal to metal, and thus so too does the treatment necessary to prevent corrosion. Noble metals such as Au and Pt group metals do not readily form oxides, whereas some metals such as Al, Ti, and Cr form a thin, self-passivating oxidized layer that serves to protect the bulk of the metal from further oxidation [101]. The oxide layers of other metals such as Cu do not protect the bulk and thus have the possibility of total corrosion. Such metals must be passivated with a stable material if they are to be exposed to the atmosphere or harsh

UNCORRECTED PROOF

conditions for long periods of time. Also, when creating contacts to these metals in successive metallization steps, the oxide should be removed immediately prior to the contact being made. Sputtering tools often feature an argon sample sputtering that can etch away the oxidized layer by ion milling. This is particularly useful, as the freshly cleaned metal surface is kept in an inert environment until sputtering the next metal.

Another important design aspect that can be easily overlooked is external connections. Most MEMS devices use bond pads on the chip surface for external electrical connections. These metal surfaces are exposed to the ambient environment, and subject to oxidation/corrosion, so exposed metals should exhibit self-passivating oxidation characteristics. It is also often desired to have metals that are easily solderable and/or wire bondable to facilitate device packaging.

3.5.3 Mechanical Properties

Although not as widespread as silicon or polysilicon, metals are also widely used for micromechanical elements such as beams, diaphragms, springs, hinges, and so on. The functionality and reliability of any mechanical structure depends heavily on the mechanical properties, requiring knowledge of elasticity, inelastic response, ultimate strength, and fatigue. For several reasons, however, mechanical properties of deposited films are one of the most problematic issues in MEMS designs.

First, the properties of microfabricated thin films can differ greatly from the bulk properties. Second, the mechanical properties of a material depend on both purity and microstructure, which for thin films can be very sensitive to film thickness and deposition conditions. Because of the planar fabrication processes used for MEMS, many films may be transversely isotropic (different properties in-plane versus out-of-plane). For these reasons, although general guidance can be obtained by examining bulk isotropic properties, these numbers are likely not replicated in thin films. And because of the process sensitivities described above, tight process control is very important for obtaining repeatable material properties.

Another complication is that there are numerous techniques used to directly or indirectly measure mechanical properties, including tension/compression tests, bending tests, indentation tests, dynamic tests, passive strain sensors, and others [102, 103]. Some of these methods are prone to large inaccuracies, and/or are only suited for extracting certain mechanical characteristics [104]. As a result, multiple test methodologies with different test structures may be necessary to measure all important mechanical properties.

Electroplated Ni and Ni alloys – used in LIGA-based fabrication – are the most widely studied metals for their micromechanical properties. Here, the electroplating conditions play an important role in the microstructure and thus mechanical properties. As compared to bulk Ni, electroplated Ni films generally show a slightly lower modulus, but much higher yield strength [103]. The elasticity of thin-film Al, Cu,

UNCORRECTED PROOF

SPB-140376 Chapter ID 3 October 29, 2010 Time: 08:22pm Proof 1

Table 3.16 Mechanical properties of bulk metals commonly used in MEMS [105]

Material	Density (kg m^{-3})	Young's modulus (GPa)	Poisson's ratio (Unitless)
Ag	10500	83	0.37
Al	2700	70	0.35
Au	19280	78	0.44
Cr	7190	279	0.21
Cu	8960	130	0.34
Ni	8910	200	0.31
Pt	21440	168	0.38
Ta	16650	186	0.34
Ti	4510	116	0.32
W	19250	411	0.28

and Au usually matches their bulk properties, but like Ni, their ultimate strength is usually higher [103].

The bulk mechanical properties for the most common metals used in MEMS are tabulated in Table 3.16. These values provide the designer a starting point from which to work. For design and fabrication, more specific information is required. The reader is encouraged to find the appropriate literature but cautioned not to assume identical results will be achieved, even if carefully recreating the process steps and conditions. A film deposited in one system may differ from a film deposited under identical conditions in a different system.

3.5.4 Thermal Properties

Metals are also widely used for thermal applications. They are often used as heat spreaders or thermal conductors, because most metals exhibit high thermal conductivity. They are also commonly employed in thermal bimorph actuators, where two materials with differing thermal coefficients of expansion (TCEs) are used to form a thermal actuator. Table 3.17 summarizes the bulk thermal properties of commonly used metals for MEMS.

Most metals tend to exhibit larger TCEs than semiconductors or dielectrics, thus enabling highly mismatched bimorph structures such as Al with SiO_2. For these actuators, the metal may also be used as a heater so that the actuation control is via electrical current. The converse side of this is that thermal mismatch can also create significant problems, such as thermally induced stress. This can be problematic, especially in packaging of mechanical systems.

Although metals generally have fairly high melting points, care must be exercised when considering high-temperature applications. Melting is usually not a concern, but, rather, diffusion or oxidation because many metals exhibit high diffusivity and propensity for oxidation. Special care, such as diffusion barriers or passivation layers, may be required to mitigate these surface interactions.

UNCORRECTED PROOF

Table 3.17 Thermal properties of bulk metals commonly used in MEMS[a] [96]

Material	Thermal coefficient of expansion (10^{-6} K^{-1})	Thermal conductivity (W m^{-1} K^{-1})	Specific heat capacity (J kg^{-1} K^{-1})	Melting point (K)
Ag	18.9	429	235	1235
Al	23.1	237	897	933
Au	14.2	317	129	1337
Cr	4.9	93.7	450	2180
Cu	16.5	401	384	1358
Ni	13.4	90.7	445	1728
Pt	8.8	71.6	133	2041
Ta	6.3	57.5	140	3290
Ti	8.6	21.9	522	1941
W	4.5	174	132	3695

[a]Thermal conductivity at 27°C; specific heat capacity at constant pressure at 25°C

3.5.5 *Magnetic Properties*

Various metal alloys are known to exhibit strong ferromagnetic behavior. These magnetically responsive materials are usually categorized as either soft or hard magnets. Hard magnetic materials exhibit a strong magnetization in the absence of an external magnetic field. Therefore, they can provide a source of magnetic field without any external power. Conversely, soft magnetic materials retain little remanent magnetization, but they can be easily magnetized in the presence of a small magnetic field. Soft and hard magnetic materials are often used together to guide and concentrate magnetic fields in specific regions.

Magnetic materials for MEMS are used in various ways. Soft magnetic materials can be used with electroplated metal coils to form on-chip inductors and transformers. More complex devices such as actuators, motors, generators, or energy harvesters can also be built using hard and/or soft magnets. These structures capitalize on the same electromechanical phenomena employed in large-scale electric machines. The magnetostrictive (magnetic field-induced strain) properties of certain alloys can also be used for direct magnetomechanical coupling. Deposition of

Table 3.18 Summary of typical properties for soft magnetic electroplated alloys [40]

Material	Saturation flux density (T)	Easy-axis Coercivity (Oe)	Resistivity (µΩ·cm)	Magnetostriction (ppm)	Film stress (MPa)
$Ni_{80}Fe_{20}$	1.0	0.2	20	< -3	100
$Ni_{45}Fe_{55}$	1.7	0.5	40	+20	160
Co–Fe–Cu	1.8–2.0	< 1		± 3	
Co–Ni–Fe	2.0–2.2	< 2	30	+3.5	115
$Ni_{20}Fe_{80}$	2.2	2.5	35	+25	240
Co–Fe	2.4–2.5	5–10		+45	845

Table 3.19 Select examples of hard magnetic films[a] [106]

Alloy	Deposition method	Integration notes	Thickness (µm)	Intrinsic coercivity H_{ci}(kA/m)	Remanence Br (T)	Energy product $(BH)_{max}$ (kJ/m^3)
Co–Ni–P	Plated	None	1–52	55–105[a]	0.06–0.1	1.3–1.8
Co–Ni–Mn–P	Plated	None	10–45	70–100	0.2–0.3	14
Co–Ni–Mn–P	Plated	0.2 T field	25	40–210	0.06–0.2	0.6–10
Co–Pt–P	Plated	(110) Si	2	370	0.6	52
Co–Pt–P	Plated	(110) Si substrate	8	330	1.0	69
FePt – $L1_0$	Sputtered	600°C anneal	6–7	446	–	124
FePt – $L1_0$	PLD	Small area	19–26	600	1.4	12–105
CoPt – $L1_0$	Plated	700°C anneal	10–16	800	0.37	–
Sm–Co	Sputtered	560°C anneal; glass/alumina substrate	3–50	1200	0.7–0.75	75–90
Sm–Co	Sputtered	400°C dep.; 750°C anneal	5	1035	0.8	140
Nd–Fe–B	Sputtered	500°C dep.; 750°C anneal	5	1280	1.4	400
Nd–Fe–B	PLD	650°C anneal; Small area	120	1000	0.55	77

[a]Coercivity H_c values, not intrinsic coercivity H_{ci}

UNCORRECTED PROOF

UNCORRECTED PROOF

magnetic alloy films is typically achieved via electroplating, sputtering, or PLD, inasmuch as good alloy control is necessary.

Selection of magnetic materials is very complex. Unfortunately, there is no universal "one-size-fits-all" perfect material for either soft or hard magnets. Rather, there are different microfabrication methods and different alloy combinations, each with advantages and disadvantages [40, 106]. For example, the higher saturation flux density soft magnetic alloys tend to have larger coercivities, and thus may not be suitable for high-frequency applications because of excessive hysteresis core losses. As another example, very high-performance hard magnets are possible, but they require high-temperature annealing, perhaps eliminating them from consideration because of process integration concerns. A thorough treatment of the design and selection of magnetic materials is beyond the scope of this chapter, but the information below provides a starting point for initial evaluation.

Soft magnetic metals are usually Ni, Fe, and Co metals and their alloys, such as Ni–Fe, Co–Fe, and Co–Ni–Fe. The properties required for soft magnetic materials are high-saturation flux density, high permeability, low coercivity, and high resistivity. In addition, low magnetostriction, low film stress, and good corrosion resistance are also desired. Table 3.18 lists typical soft magnetic electroplated alloys and their properties. $Ni_{80}Fe_{20}$ is the most widely used because of its good magnetic performance and relatively easy and reliable fabrication.

Hard magnetic metals include some transition metal alloys (e.g., Co–Ni–P, Co–P, Fe–Pt, and Co–Pt) and iron/cobalt-rich rare-earth intermetallics (e.g., $SmCo_5$, Sm_2Co_{17}, $Nd_2Fe_{14}B$). Hard magnets generally serve as a source of magnetic field, therefore the performance required for hard magnets are high energy density, high coercivity, and high remanence, as well as good thermal and chemical stability. Table 3.19 summarizes selected hard magnetic metal alloys. Co–Ni alloys are the most widely explored. They can be easily electroplated at low temperatures, but the magnetic properties are fairly weak. Electroplated Co-rich Co–Pt alloys (Co content approximately 80%) have also been developed with better performance. Equiatomic CoPt and FePt alloys have also been demonstrated with even better performance, but high-temperature annealing is required to induce an ordered $L1_0$ phase. Sputtered rare-earth alloys of Sm–Co or Nd–Fe–B offer the strongest properties (as in bulk), but these all require high-temperature deposition or annealing.

References

1. S.A. Campbell: Fabrication Engineering at the Micro- and Nanoscale, Ch. 12 (Oxford University Press, New York, NY, 2008)
2. D.B. Fraser: Metallization in VLSI Technology, S.M. Sze (Ed.) (McGraw-Hill, New York, NY, 1983)
3. R.J. Gnaedinger: Some calculations of the thickness distribution of films deposited from large area sputtering sources, J. Vac. Sci. Technol. 6, 355–362 (1969)
4. I.A. Blech, H.A. Vander Plas: Step coverage simulation and measurements in a DC planar magnetron sputtering systems, J. Appl. Phys. 54, 3489–3496 (1983)
5. Y.H. Park, F.T. Zold, J.F. Smith: Influences of DC bias on aluminum films prepared with a high rate magnetron sputtering cathode, Thin Solid Films 129, 309–314 (1985)

6. S. Kobayashi, M. Sakata, K. Abe, T. Kamei, O. Kasahara, H. Ohgishi, K. Nakata: High rate deposition of $MoSi_2$ films by selective co-sputtering, Thin Solid Films 118, 129–138 (1984)
7. D.H. Weon, J.I. Kim, S. Mohamadi: Design of high-Q 3-D integrated inductors for high frequency applications, Analog Integr. Circuits Signal Process. 50, 89–93 (2007)
8. M. Ataka, A. Omodaka, N. Takeshima, H. Fujita: Fabrication and operation of polyimide bimorph actuators for a ciliary motion system, J. Microelectromech. Syst. 2, 146–150 (1993)
9. M. Schlesinger, M. Paunovic: Modern Electroplating (Wiley, New York, NY, 2000)
10. D.R. Crow: Principles and Applications of Electrochemistry (Stanley Thornes (Publishers) Ltd., Cheltenham, 1998)
11. M. Paunovic, M. Schlesinger: Fundamentals of Electrochemical Deposition (Wiley, New York, NY, 1998)
12. D. Landolt: Electrochemical and materials science aspects of alloy deposition, Electrochim. Acta 39, 1075–1090 (1994)
13. H. Löwe, W. Ehrfeld, J. Schiewe: Micro-Electroforming of Miniaturized Devices for Chemical Applications, In J.W. Schultze et al. (Eds.): Electrochemical Microsystem Technologies, pp. 245–268 (Taylor & Francis, New York, NY, 2002)
14. T. Fritz: Charakterisierung galvanisch abgeschiedener Nickel- und Nickelwolframschichten für mikrotechnische Anwendungen, Dissertation D82 RWTH Aachen (2002)
15. A. Gemmler, W. Keller, H. Richter, H. Ruess: Mikrostrukturen- Prozesswissen erlaubt höchste Präzision (English: Micro devices – process models for high precision), Metalloberfläche 47, 461–468 (1993)
16. J.C. Puippe: Theory and Practice of Pulse Plating (American Electroplaters and Surface Finishers Society, Orlando, FL, 1986)
17. R.K. Sharma, A.C. Rastog, K. Jain, G. Singh: Microstructural investigations on CdTe thin films electrodeposited using high current pulses, Physica B 366, 80–88 (2005)
18. W. Wang, F.Y. Hou, H. Wang, H.T. Guo: Fabrication and characterization of Ni–ZrO2 composite nano-coatings by pulse electrodeposition, Scr. Mater. 53, 613–618 (2005)
19. M.V. Rastei, S. Colis, J.P. Bucher: Growth control of homogeneous pulsed electrodeposited Co thin films on n-doped Si(111) substrates, Chem. Phys. Lett. 417, 217–221 (2005)
20. F. Lallemand, L. Ricq, E. Deschaseau, L. De Vettor, P. Bercot: Electrodeposition of cobalt-iron alloys in pulsed current from electrolytes containing organic additives, Surf. Coat. Technol. 197, 10–17 (2005)
21. E. Becker, W. Ehrfeld, P. Hagmann, A. Maner, D. Münchmeyer: Fabrication of microstructures with high aspect ratios and great structural heights by synchrotron radiation lithography, galvanoforming, and plastic molding (LIGA process), Microelectron. Eng. 35, 35–56 (1986)
22. S. Harsch, W. Ehrfeld, A. Maner: Untersuchungen zur Hrestellung von Mikrostrukturen großer Strukturhöhe durch Galvanoformung in Nickelsulfamatelektrolyten, Reserach Centre Karlsruhe, Germany, Report No. 4455 (1988)
23. W. Stark, M. Saumer, B. Matthis: Nickelsulfamat-Elektrolyte für die Mikrogalvanoformung, Galvanotechnik 86, 1107–111 (1996)
24. M. Guttmann, J. Schulz, V. Saile: Lithographic Fabrication of Mold Inserts, In H. Baltes, O. Brand, G.K. Fedder, C. Hierold, J. Korvink, O. Tabata (Eds.): Advanced Micro and Nanosystems, Vol. 3: Microengineering of Metals and Ceramics, Ch. 8 (Wiley-VCH, Weinheim, 2005)
25. T. Fritz, M. Griepentrog, W. Mokwa, U. Schnakenberg: Determination of Young's modulus of electroplated nickel, Electrochim. Acta 48, 3029–3035 (2003)
26. W. Bacher, K. Bade, K. Leyendecker, W. Menz, W. Stark, A. Thommes: Electrodeposition of Microstructures, In N. Masuko, T. Osaka, Y. Ito (Eds.): Electrochemical Technology, Ch. 9, pp. 159–189 (Gordon and Breach, Kodansha, 1996)
27. R. Ruprecht, W. Bacher: Mikrogalvanoformung für die Weltraumforschung – Herstellen von Infrarotfiltern (English: Micro-galvanoforming for space research – production of infra-red filters), Metalloberfläche 45, 531–534 (1991)

UNCORRECTED PROOF

28. P.M. Vereecken, R.A. Binstead, H. Deligianni, P.C. Andricacos: The chemistry of additives in damascene copper plating, IBM J. Res. Dev. 49, 1–18 (2005)
29. T. Osaka, Y. Okinaka, J. Sasano, M. Kato: Development of new electrolytic and electroless gold plating processes for electronics applications, Sci. Technol. Adv. Mater. 7, 425–437 (2006)
30. H. Honma, K. Hagiwara: Fabrication of gold bumps using gold sulfite plating, J. Electrochem. Soc. 142, 81–87 (1995)
31. J.J. Kelly, N. Yang, T. Headley, J. Hachmann: Experimental study of the microstructure and stress of electroplated gold for microsystem applications, J. Electrochem. Soc. 150, C445–C450 (2003)
32. N. Dambrowsky, J. Schulz: Gold plating in microsystem technology – challenges by new applications (original: Goldgalvanik in der Mikrosystemtechnik – Herausforderungen durch neue Anwendungen), Scientific Report FZKA 7308, Forschungszentrum Karlsruhe GmbH, Karlsruhe (2007)
33. M.J. Liew, S. Roy, K. Scott: Development of a non-toxic electrolyte for soft gold electrodeposition: An overview of work at University of Newcastle upon Tyre, Green Chem. 5, 376–381 (2003)
34. Y. Okinaka, M. Hoshino: Some recent topics in gold plating for electronics applications, Gold Bull. 31, 3–13 (1998)
35. A. Maner, W. Ehrfeld, R. Schwarz: Electroforming of absorber patterns of gold on masks for X-ray lithography, Galvanotechnik 79, 1101–1106 (1988)
36. A. Brenner: Electrodeposition of Alloys: Principles and Practice, Volumes I and II (Academic, New York, NY, 1963)
37. D. Landolt, A. Marlot: Microstructure and composition of pulse-plated metals and alloys, Surf. Coat. Technol. 169–170, 8–13 (2003)
38. P.C. Andricacos, L.T. Romankiw: Magnetically Soft Materials in Data Storage: Their Properties and Electrochemistry, In H. Gerischer, C.W. Tobias (Eds.): Advances in Electrochemical Science and Engineering, pp. 230–321 (VCH, Weinheim, 1994)
39. T. Budde, M. Föhse, B. Majjer, H. Lüthje, G. Bräuer, H.H. Gatzen: An investigation on technologies to fabricate magnetic microcomponents for miniaturized actuator systems, Microsyst. Technol. 10, 237–240 (2004)
40. E.I. Cooper, C. Bonhôte, J. Heidmann, Y. Hsu, P. Kern, J.W. Lam, M. Ramasubramanian, N. Robertson, L.T. Romankiw, H. Xu: Recent developments in high-moment electroplated materials for recording heads, IBM J. Res. Dev. 49, 103–126 (2005)
41. M. Föhse: Entwurf und Fertigung eines linearen elektromagnetischen Mikromotors nach dem Synchronprinzip, Dissertation, Universität Hannover (2005)
42. U. Kirsch, R. Degen: Hochpräzise und wirtschaftlich – Die Galvanoformung als hochpräzises Verfahren zur Abformung von Mikrozahnrädern, Metalloberfläche 61, 33–35 (2007)
43. T. Kohlmeier, V. Seidemann, S. Büttgenbach, H.H. Gatzen: An investigation on technologies to fabricate microcoils for miniaturized actuator systems, Microsyst. Technol. 10, 175–185 (2004)
44. S. Roy, A. Connell, A. Ludwig, N. Wang, T. O'Donnell, M. Brunet, P. McCloskey, C. Ómathúna, A. Barman, R.J. Hicken: Pulse reverse plating for integrated magnetics on Si, J. Magn. Magn. Mater. 290–291, 1524–1527 (2005)
45. Y. Sverdlow, Y. Rosenberg, Y.I. Rozenberg, R. Zmood, R. Erlich, S. Natan, Y. Shacham-Diamand: The electrodeposition of cobalt-nickel-iron high aspect ratio thick film structures for magnetic MEMS applications, Microelectron. Eng. 76, 258–265 (2004)
46. F.E. Rasmussen, J.T. Ravnkilde, P.T. Tang, O. Hansen, S. Bouwstra: Electroplating and characterization of cobalt-nickel-iron and nickel-iron for magnetic microsystems applications, Sens. Act. A Phys. 92, 242–248 (2001)
47. P.T. Tang: Pulse reversal plating of nickel and nickel alloys for MEMS. Proceedings SUR/FIN, Nashville, June 25–28, pp. 224–232 (2001)

AQ5

48. J.O. Dukovic: Current Distribution and Shape Change in Electrodeposition of Thin Films for Microelectronic Fabrication, In Advances in Electrochemical Science and Engineering, pp. 119–157 (Verlag Chemie, Weinheim, 1994)
49. L.T. Romankiw, D.A. Herman, Proceedings of the Fourth International Symposium on Magnetic Materials, Processes and Devices, pp. 626–636 (The Electrochemical Society, Pennington, NJ, 1995)
50. A. Thommes, W. Stark, W. Bacher: Die galvanische Abscheidung von Eisen-Nickel in LIGA-Mikrostrukturen. Scientific Reports, Research Centre Karlsruhe FZKA 5586 (1995)
51. S. Abel: Charakterisierung von Materialien zur Fertigung elektromagnetischer Mikroaktoren in LIGA Technik. Dissertation, University of Kaiserslautern, Germany (1996)
52. S.D. Leith, S. Ramli, D.T. Schwartz: Characterization of Ni_xFe_{1-x} (0.10<x<0.95) electrodeposition from a family of sulfamate-chloride electrolytes, J. Electrochem. Soc. 146, 1421–1435 (1999)
53. U. Kirsch: Elektrochemische Abscheidung von spannungsarmen Nickel-Eisen-Legierungsschichten und ihre Eigenschaften für Bauteile der Mikrosystemtechnik, Dissertation, University of Freiburg (Klaus Bielefeld Verlag, Friedland, 2000)
54. D.L. Grimmet, M. Schwartz, K. Nobe: Pulsed electrodeposition of iron-nickel alloys, J. Electrochem. Soc. 134, 3414–3418 (1990)
55. C. Müller, M. Sarret, T. Andreu: ZnMn alloys obtained using pulse, reverse and superimposed current modulations, Electrochim. Acta 48, 2397–2404 (2003)
56. J.Y. Fei, G.D. Wilcox: Electrodeposition of Zn–Co alloys with pulse containing reverse current, Electrochim. Acta 50, 2693–2698 (2005)
57. F. Giro, K. Bedner, C. Dhum, J.E. Hoffmann, S.P. Heussler, J. Linke, U. Kirsch, M. Moser, M. Saumer: Pulsed electrodeposition of high aspect-ratio NiFe assemblies and its influence on spatial alloy composition, Microsyst. Technol. 14, 1111–1115 (2008)
58. A. Brenner, G.E. Riddell: Nickel plating on steel by chemical reduction, United States Bureau of Standards, J. Res. 37, 31–34 (1946)
59. J.G. Jin, S.K Lee, Y.H Kim: Adhesion improvement of electroless plated Ni layer by ultrasonic agitation during zincating process, Thin Solid Films 466, 272–278 (2004)
60. F. Touyeras, J.Y. Hihn, X. Bourgoin, B. Jacques, L. Hallez, V. Branger: Effects of ultrasonic irradiation on the properties of coatings obtained by electroless plating and electro plating, Ultrasonics Sonochem. 12, 13–19 (2004)
61. F.A. Lowenheim (Ed.): Modern Electroplating, 3rd edn, Ch. 31 (Wiley, New York, NY, 1974)
62. A. Brenner, G. Riddell: Deposition of nickel and cobalt by chemical reduction, United States Bureau of Standards, J. Res. 39, 385–395 (1947)
63. A. Brenner: Electroless plating comes of age, Metal Finish. 52, 61–68 (1954)
64. N. Feldstein, T.S. Lancsek: Selective electroless plating by selective deactivation, RCA Rev. 31, 439–442 (1970)
65. T. Berzins: Alloy and Composite Metal Plate, U.S. Patent 3,045,334 (1962)
66. R.M. Hoke: Chemical Plating of Metal-Boron Alloys, U.S. Patent 2,990,296 (1961)
67. G.O. Mallory, J.B. Hajdu (Eds.): Electroless Plating Fundamentals and Applications, American Electroplaters and Surface Finishers Society (Noyes Publications/William Andrew Publishing, LLC, New York, NY, 1990)
68. A. Hung, K.-M. Chen: Mechanism of hypophosphite-reduced electroless copper, J. Electrochem. Soc. 136, 72–75 (1989)
69. P. Fintschenko, E.C. Groshart: Electroless copper plating, Metal Finish. 68, 85–87 (1970)
70. A.E. Cahill: Surface catalyzed reduction of copper, Proc. Am. Electroplaters' Soc. 44, 130 (1957)
71. O.B. Dutkewych, Electroless Copper Plating, U.S. Patent 3,475,186 (1969)
72. Y. Okinaka, In G.O. Mallory, J.B. Hajdu (Eds.), Electroless Plating of Gold and Gold Alloys, Ch. 11, American Electroplaters and Surface Finishers Society (Noyer Publications/William Andrew Publishing, New York, NY, 1990)
73. J.F. McCormack: Autocatalytic Gold Plating Solutions, U.S. Patent 3,589,916 (1971)

UNCORRECTED PROOF

2386 74. S. Mehdizadeh, J.O. Dukovic, P.C. Andricacos, L.T. Romankiw: The influence of lithographic patterning on current distribution: A model for microfabrication by electrodeposition, J. Electrochem. Soc. 139, 78–91 (1992)
2388 75. J.K. Luo, D.P. Chu, A.J. Feewitt, S.M. Spearing, N.A. Fleck, W.I Milne: Uniformity control of Ni thin film microstructures deposited by through mask plating, J. Electrochem. Soc. 152, C36–C41 (2005)
2391 76. K. Leyendecker: Untersuchungen zum Stofftransport bei der Galvanoformung von LIGA-Mikrostrukturen, Dissertation, Universität Karlsruhe (1995)
2393 77. U. Gengenbach, I. Sieber, U. Wallrabe: Design for LIGA and Safe Manufacturing, In O. Brand, G. Fedder, C. Hierold, J. Korvink, O. Tabata (Eds.): Advanced Micro & Nanosystems, Vol. 7: LIGA and Its Applications, pp. 143–188 (Wiley-VCH, Weinheim, 2009)
2396 78. V. Saile, U. Wallrabe, O. Tabata: LIGA and Its Applications (Wiley-VCH, Weinheim, 2009)
2397 79. W. Menz, J. Mohr, O. Paul: Microsystem Technology, Ch. 7: The LIGA Process, p. 289 (Wiley VCH, Weinheim, 2001)
2399 80. Y.J. Kim, M.G. Allen: Surface micromachined solenoid inductors for high frequency applications, IEEE Trans. Compon. Packaging Manuf. Technol. C 21, 26–33 (1998)
2401 81. J.Y. Park, M.G. Allen: High *Q* spiral-type microinductors on silicon substrates, IEEE Trans. Magn. 135, 3544–3546 (1999)
2403 82. J.-B. Yoon, C.H. Han, E. Yoon, C.K. Kim: Monolithic high-*Q* overhang inductors fabricated on silicon and glass substrates. Technical Digest of IEEE International Electron Devices Meeting, Dec. 5–8, 1999, pp. 753–756 (1999)
2405 83. B. Morgan, X. Hua, T. Iguchi, T. Tomioka, G.S. Oehrlein, R. Ghodssi: Substrate interconnect technologies for 3-D MEMS packaging, Microelectron. Eng. 81, 106–116 (2005)
2407 84. Y.K. Yoon, M.G. Allen: Embedded conductor technology for micromachined RF elements, J. Micromech. Microeng. 15, 1317–1326 (2005)
2409 85. P. Gwynne: Back to the future: Copper comes of age, IBM Res. 35, 17–21 (1997)
2410 86. F. Cros, K. Kim, M.G. Allen: A single-mask process for micromachined magnetic devices. Proceedings of the Solid State Sensor and Actuator Workshop (Hilton Head Island, SC), pp. 138–141 (1997)
2412 87. J.A. Thornton, D.W. Hoffman: Stress-related effect in thin films, Thin Solid Films 171, 5–31 (1989)
2414 88. M.K. Ghosh, K.L. Mittal (Eds.): Polyimides: Fundamentals and Applications, Ch. 20–21 (Marcel Dekker, New York, NY, 1996)
2416 89. F.K. LeGoues, B.D. Silverman, P.S. Ho: The microstructure of metal-polyimide interfaces, J. Vac. Sci. Technol. A 6, 2200–2204 (1988)
2417 90. N. Bowden, S. Brittain, A.G. Evans, J.W. Hutchinson, G.M. Whitesides: Spontaneous formation of ordered structures in thin films of metals supported on an elastomeric polymer, Nature 393, 146–149 (1998)
2420 91. G. Jia, M.J. Madou: MEMS Fabrication, In M. Gad-el-Hak (Ed.): The MEMS Handbook, 2nd edn, Vol. 2: MEMS Design and Fabrication, pp. 3–114 (CRC Press/Taylor and Francis, Boca Raton, FL, 2006)
2422 92. K.L. Mittal (Ed.): Adhesion Aspects of Thin Films, Vol. 2, p. 125 (VSP, Utrecht, 2005)
AQ6 2423 93. C.K. Hu, M.B. Small, F. Kaufman, D.J. Pearson, In S.S. Wong, S. Furuka (Eds.): Tungsten and Other Advanced Metals for VLSI/ULSI Applications, p. 369 (Materials Research Society, Pittsburgh, PA, 1989)
2426 94. D.R. Lide (Ed.): CRC Handbook of Chemistry and Physics, 90th edn (CRC Press/Taylor and Francis, Boca Raton, FL, 2008). Internet Version available: http://www.hbcpnetbase.com/
2427 95. G.T.A. Kovacs: Micromachined Transducers Sourcebook, p. 561 (McGraw Hill, Boston, MA, 2006).
AQ7 2429 96. J.R. Davis(Ed.): Base-Metal Selection, In Metals Handbook Desk Edition, 2nd edn (ASM International, Materials Park, OH, 1998)

2431 97. S.K. Prasad: Advanced Wirebond Interconnection Technology (Kluwer, Bangalore, 2004)
2432 98. G.G. Harman: Wire Bonding in Microelectronics, 2nd edn (McGraw Hill, New York, NY, 1997)
2433 99. S.D. Cramer, B.S. Covino (Eds.): ASM Handbook, Vol. 13B: Corrosion: Materials (ASM International, 2005)
2435 100. D. Jiles: Introduction to Magnetism and Magnetic Materials, 2nd edn, Ch. 2, 4 (CRC Press/Taylor and Francis, Boca Raton, FL, 1998)
2437 101. T.W. Swaddle: Inorganic Chemistry: An Industrial and Environmental Perspective, p. 104 (Academic, San Diego, CA, 1997)
2438 102. T. Yi, C.J. Kim: Measurement of mechanical properties of MEMS materials, Measurement Sci. Technol. 10, 706–717 (1999)
2440 103. W.N. Sharpe: Mechanical Properties of MEMS Materials, In M. Gad-el-Hak (Ed.): The MEMS Handbook, 2nd edn, Vol. 1: MEMS Introduction and Fundamentals, Ch. 3 (CRC Press/Taylor & Francis, Boca Raton, FL, 2006)
2443 104. V.T. Srikar, S.M. Spearing: A critical review of microscale mechanical testing methods used in the design of microelectromechanical systems, Exp. Mech. 43, 238–247 (2006)
AQ8 2444 105. M. Winter: WebElements: the periodic table on the web (2009). Available at http://www.webelements.com/
AQ9 2446 106. D.P. Arnold, N. Wang: Permanent magnets for MEMS. J. Microelectromech. Syst. 18, 1255–1266

2448 2449 2450 2451 2452 2453 2454 2455 2456 2457 2458 2459 2460 2461 2462 2463 2464 2465 2466 2467 2468 2469 2470 2471 2472 2473 2474 2475

UNCORRECTED PROOF

2476 # Chapter 3

Q. No.	Query
AQ1	“D.P. Arnold” has been set as corresponding author. Please check.
AQ2	Please provide citation for Table 3.10.
AQ3	Please provide page range and chapter title for reference [2].
AQ4	Please provide the page range for reference [24].
AQ5	Please provide the editor names for reference [48].
AQ6	Please provide the chapter title for reference [93].
AQ7	Please provide the editor name and page range for reference [96].
AQ8	Please provide the accessed date for reference [105].
AQ9	Please provide the year for reference [106].

2477 2478 2479 2480 2481 2482 2483 2484 2485 2486 2487 2488 2489 2490 2491 2492 2493 2494 2495 2496 2497 2498 2499 2500 2501 2502 2503 2504 2505 2506 2507 2508 2509 2510 2511 2512 2513 2514 2515 2516 2517 2518 2519 2520

UNCORRECTED PROOF